# Advance of Sustainable Energy Materials: Technology Trends for Silicon-Based Photovoltaic Cells

**Article** *in* Sustainability · September 2024

DOI: 10.3390/su16187962



**1 author:**

Mladen Bošnjaković
University of Slavonski Brod
**59** PUBLICATIONS **508** CITATIONS

SEE PROFILE

*sustainability*

MDPI

*Review*

# Advance of Sustainable Energy Materials: Technology Trends for Silicon-Based Photovoltaic Cells

**Mladen Bošnjaković**

Technical Department, University of Slavonski Brod, Trg Ivane Brlić Mažuranić 2, 35000 Slavonski Brod, Croatia; mbosnjakovic@unisb.hr

**Abstract:** Modules based on c-Si cells account for more than 90% of the photovoltaic capacity installed worldwide, which is why the analysis in this paper focusses on this cell type. This study provides an overview of the current state of silicon-based photovoltaic technology, the direction of further development and some market trends to help interested stakeholders make decisions about investing in PV technologies, and it can be an excellent incentive for young scientists interested in this field to find a narrower field of research. This analysis covers all process steps, from the production of metallurgical silicon from raw material quartz to the production of cells and modules, and it includes technical, economic and environmental aspects. The economic aspect calls for more economical production. The ecological aspect looks for ways to minimise the negative impact of cell production on the environment by reducing emissions and using environmentally friendly materials. The technical aspect refers to the state of development of production technologies that contribute to achieving the goals of the economic, environmental and sustainability-related aspects. This involves ways to reduce energy consumption in all process steps, cutting ingots into wafers with the smallest possible cutting width (less material waste), producing thin cells with the greatest possible dimensional accuracy, using cheaper materials and more efficient production. An extremely important goal is to achieve the highest possible efficiency of PV cells, which is achieved by reducing cell losses (optical, electrical, degradation). New technologies in this context are Tunnel Oxide Passivated Contact (TOPcon), Interdigitated Back Contact Cells (IBCs), Heterojunction Cells (HJTs), Passivated Emitter Rear Totally Diffused cells (PERTs), silicon heterojunction cells (SHJs), Multi-Bush, High-Density Cell Interconnection, Shingled Cells, Split Cells, Bifacial Cells and others. The trend is also to increase the cell size and thus increase the output power of the module but also to reduce the weight of the module per kW of power. Research is also focused to maximise the service life of PV cells and minimise the degradation of their operating properties over time. The influence of shade and the increase in cell temperature on the operating properties should preferably be minimised. In this context, half-cut and third-cut cell technology, covering the cell surface with a layer that reduces soiling and doping with gallium instead of boron are newer technologies that are being applied. All of this leads to greater sustainability in PV technology, and solar energy becomes more affordable and necessary in the transition to a "green" economy.

**Keywords:** photovoltaic; wafer; encapsulation; backsheet; busbar; monocrystalline Si



**Citation:** Bošnjaković, M. Advance of Sustainable Energy Materials: Technology Trends for Silicon-Based Photovoltaic Cells. *Sustainability* **2024**, *16*, 7962. https://doi.org/10.3390/su16187962

Academic Editors: Alevtrina (Alla) White Smirnova and Firoz Alam

Received: 21 June 2024
Revised: 15 August 2024
Accepted: 10 September 2024
Published: 12 September 2024



## 1. Introduction

The development of silicon-based photovoltaic (PV) cells began with the discovery of the photovoltaic effect by Alexandre-Edmond Becquerel in 1839. The first practical application of this effect was realised in 1883 when Charles Fritts created the first solar cell using the semiconductor selenium and a thin layer of gold to create junctions with an efficiency of only about 1%. In 1954, Bell Labs introduced the first modern silicon-based PV cell with an efficiency of around 4% [1]. Since then, continuous research and development efforts have led to significant improvements in the efficiency and production of PV cells. In the 1960s and 1970s, research focused on improving silicon purity and optimising

manufacturing processes, which led to higher PV cell efficiency. With the introduction of techniques such as boron diffusion and anti-reflective coatings, the efficiency of the cells was gradually increased further.

In the 1980s and 1990s, the technology for manufacturing silicon-based photovoltaic cells (PV cells) underwent significant changes that increased their efficiency and reduced production costs. One of the most important improvements was the introduction of silicon purification techniques that resulted in a higher quality semiconductor material with fewer impurities, which had a direct impact on increasing the efficiency of PV cells. In addition, new methods for producing thinner silicon layers were developed, which enabled a reduction in material costs and facilitated the integration of PV cells into various products and structures.

At the same time, innovations in cell design, such as the use of surface textures that reduce light reflection and increase absorption, have contributed to greater efficiency in the conversion of light energy into electricity. The introduction of passivation layers on the back of the cells also reduced energy losses due to the recombination of charge carriers, which further improved performance. In the 2000s, standard silicon cells achieved efficiencies of around 15–20%.

In addition, the development of new techniques for connecting the cells in the module enabled better mechanical stability and longevity of the PV module. In the first decade of the 21st century, PV cell manufacturing technology evolved significantly. Greater automation, quality control and lower energy consumption have led to advances in production processes, resulting in more efficient production lines and better-quality PV modules.

Today, silicon PV cells dominate the market due to their reliability, longevity and increasing efficiency, which is why this analysis focuses on them. As technological innovations continue to reduce costs and increase availability and sustainability, silicon PV cells remain a key player in the global transition to renewable energy.

Some technologies such as additive technologies and artificial intelligence will certainly contribute to the development of PV cells, but for space reasons they are not analysed here.

The introductory part usually provides an overview of the main research results available in the literature, which is not the case here. The approach is different. In each chapter, the scientific research on the topic in question is listed with an analysis of possible improvements to existing processes. As the analysis covers all process steps of production, from the extraction of metallurgical silicon from quartz raw material to the production of PV modules, the amount of the literature cited is considerable. In addition, the author presents his views directly or indirectly. In conclusion, the analysis covers all important aspects, i.e., technical, economic and environmental aspects, as well as aspects of sustainability.

The aim of this study is to provide an overview of the current development status of Si-based PV cell technology, the latest PV cell technologies on the market, research and development directions and some market trends, which can help all interested stakeholders in making decisions about investing in PV technologies. Likewise, this analysis can be an excellent basis for young researchers who are interested in this field to find a narrower research area.

## 2. Materials and Methods

This analysis is based on a process approach, which means that all processes related to the production of PV cells and modules were analysed, starting with obtaining metallurgical grade silicon (MG-Si) from quartz raw materials. The processes that follow are obtaining solar-grade silicon (SG-Si) and the production of mono- or polycrystalline silicon (ingots) with a good crystallographic structure. The ingots are then cut into thin wafers from which the PV cells are then manufactured. A number of processes must be carried out to produce PV cells from wafers (texturing the surface, applying an anti-reflective coating, passivation, attaching metal contacts, etc.). With the aim of increasing the efficiency of the cells, various solutions are being proposed to reduce the losses in the cell, which is gradually leading to a

number of new technologies coming onto the market, such as Passivated Emitter Rear Cells (PERCs), Tunnel Oxide Passivated Contact (TOPCon), Interdigitated Back Contact Cells (IBCs), Heterojunction Cells (HJTs), Bifacial Cells and Multi-Bushbar Cells. However, this is not the end of the story, as the cells are then stacked to form a module in order to achieve higher output power. The efficiency of the module is lower than the efficiency of the cells, as there are certain losses associated with the construction of the module and the exposure of the module to environmental influences. These losses should also be reduced, which is why certain improvements are proposed, such as half-cut and 1/3-cut cells, shingled cells and gapless cells. The materials used to assemble the cells into the module are also important, e.g., EPA, backsheet, etc. In addition to technical properties, the costs of these materials, ecological properties and the sustainability aspect are also important so that new materials and new technologies can also be developed in this area. In general, it can be said that information on the prevailing processes and alternative processes is provided for each production stage. In addition to the economic analysis, which usually includes energy and material costs, the impact on the environment is also taken into account. For the overall analysis, numerous relevant literature sources were consulted, most of which can be found in scientific bibliographic databases such as WoS, Scopus, PubMed, Google Scholar, open-access repositories such as ResearchGate and HAL but also data from specialised institutions dealing with energy and current information from trade journals dealing with the PV industry. In addition, the author also presents his observations and assessments on the further development of PV technologies.

## 3. Results and Discussion

### *3.1. Production of Metallurgical Silicon*

The first step in the production process of polysilicon is the extraction of quartz from the silicon mine. This is followed by the comminution and purification of the quartz material using mechanical and chemical methods. Quartz should contain 98–99% $SiO_2$. Quartz should contain less than 0.06 per cent impurities of Al, Ca and K. The impurity content of titanium should be <50 ppm, iron should be <0.1%, phosphorus should be <0.001% and sodium should be <0.01%. Impurities of iron and transition elements become sources of defects in the cell and impair the performance of the solar cell, which is why they are listed in the ppm range. Boron and phosphorus are dopants for p-type and n-type cells and interfere with and negatively affect the operation of PV cells. Therefore, their permissible content is set in the order of parts per million (ppm).

The next step is the production of metallurgical silicon (MG-Si) from quartz raw material in large industrial furnaces. They consume large amounts of electricity, around 10–13 MWh, to produce one tonne of MG-Si [2–4]. Energy consumption depends on several factors, like the type of furnace, its nominal capacity and the proportions of raw materials used [5,6].

The optimisation of energy consumption in silicon production includes various strategies such as the following [7,8]:

- The use of different carbonaceous materials, which can reduce energy consumption per unit (e.g., overall energy efficiency can be improved by adding wood crisps to a mixture of carbonaceous materials. The use of coffee husks as an additive in silicon melting also stabilises the working conditions in the furnace);
- Optimisation of the proportion of raw materials, which significantly influences the specific energy consumption and exergy efficiency of the process;
- Improvement of the efficiency of the furnace in terms of its design.

The recycling of PV modules for silicon production can also contribute to reducing energy consumption and thus $CO_2$ emissions, depending on how much energy is required to process the recycled silicon material to the appropriate quality for wafers [2,9].

The quartz is fed into the furnace together with the carbon source, which is a mixture of coal, coke, wood crisps or charcoal.

The mixture is then heated to around 2000 °C together with the quartz. The MG-Si is discharged at the furnace bottom and then solidified in the bed casting process. This is followed by the processes of purifying, crushing and packaging.

The exergy lost during the combustion of by-product gases and the exergy lost with the exhaust gas from the furnace contribute the most to low thermodynamic process efficiency. It is therefore necessary to work on the maximum utilisation of the thermal exergy of the exhaust gas in the process itself, which significantly improves the efficiency of the process [4].

The purity of the MG-Si obtained with this process is approx. 98% [10] and depends mainly on the purity of the raw materials used in the process. The major impurities in MG-Si that affect the performance of solar cells are boron, carbon, aluminium and iron. To improve the quality of MG-Si, the iron impurities in the coal must be removed [11].

Effectively reducing metal impurities in MG-Si is extremely important, so it is not surprising that much research is being carried out in this area [12–17].

Recently, several alternative methods for extracting MG-Si have been tested. The SisAl pilot project, for instance, uses secondary raw materials such as aluminium scrap and slag to replace current carbon reducers in order to demonstrate a patented new industrial process for the production of silicon based on aluminothermic reduction in quartz in slag. The new smelting process also makes better use of the raw material (quartz) [18,19].

### *3.2. Production of Solar Grade Silicon*

For the production of solar cells, the purity of solar grade Si (SG-Si) must be 99.9999% (grade 6 N). The electronics industry requires an even higher degree of purity, around 9–11 N, for the production of integrated circuits [20]. On an industrial scale, SG-Si is produced by converting MG-Si into a volatile silicon compound, which is then purified and broken down into elemental silicon.

Despite the fact that there are numerous SG-Si manufacturing techniques and patents, four main industrial processes for the production of SG-Si should be mentioned. These are the Siemens process, the Union Carbide process, the Wacker process and the Ethyl Corporation process [21]. Of these, only two processes have a significant market share: the Siemens process with a share of over 90% and the fluidised bed reactor process with a share of 3–5% [20,22].

#### 3.2.1. Siemens Process

The chemical vapour deposition (CVD) of silicon from trichlorosilane in a rod reactor is the key step in the Siemens method [23]. This process is very energy-intensive.

Trichlorosilane, often referred to as $SiHCl_3$ or TCS for short, is a highly volatile liquid obtained in a process that begins with reduction in quartz in an electric arc furnace to produce MG-Si. This liquid is used in the Siemens process to remove the 0.5 to 1.5% impurities in MG-Si.

For this purpose, MG-Si is crushed into tiny fragments that react with hydrogen chloride (HCl). The formed TCS has a low boiling point of 31.8 °C, making it relatively easy to purify in high distillation columns.

The TCS then deposits Si onto thin silicon filaments that are heated to 1050 °C to 1150 °C in a steel bell reactor until they grow into polysilicon rods that are 15 to 20 cm in diameter. The long rods are then broken into small pieces.

The Siemens process can produce 1 tonne of polysilicon and 15–20 tonnes of silicon tetrachloride ($SiCl_4$ or STC for short) as a by-product, which is liquid at room temperature and cannot be easily stored or transported. The by-product STC is mainly recycled in TCS by hydrochlorination and fed back into the system as a raw material [24,25]. The primary benefit of the Siemens process is that it is a well-established technology that can be used to produce high-purity silicon (usually more than 9 N). The Siemens process is relatively easy to handle and has proven to be very reliable [25].

Since its invention, the Siemens process has made enormous progress in reducing production costs. The top producers of polysilicon have recently reduced production costs (excluding depreciation) to below USD 10 per kilogramme of Si [26] so that its market share in polysilicon production remains dominant, mainly due to low-cost factories in China [27]. It is estimated that the polysilicon processed by Siemens accounts for 98% of market share. Production efficiency has reportedly improved, and the energy consumption of the entire solar Si production process has decreased from 66.5 kWh/kg in 2020 to 63 kWh/kg equivalent for electricity and steam in 2021 [20,28].

Of the total direct costs of SG-Si production, around 20% is accounted for by the basic raw material (MG-Si), 25% by other materials, 12% by energy, 12% by employee labour, 10% by plant maintenance and 21% by 10-year depreciation [18]. The amount of the individual costs depends on the regional location of production.

The authors believe that a further reduction in the price of SG-Si is possible by reducing energy consumption in the Siemens process through better utilisation of waste heat, reducing input costs for MG-Si and other materials, recycling $H_2$, HCl, chlorosilane, etc. and further automating the process to reduce the amount of human labour. Other points are not expected to reduce costs; on the contrary, costs could even increase. He and others have similar thoughts [29].

#### 3.2.2. The Union Carbide Process (Fluidized Bed Reactor Process or FBR)

The form of a fluidized bed reactor is tube-like. Silane ($SiH_4$) and hydrogen ($H_2$) are injected through nozzles at the bottom of the reactor to create a fluidised bed containing microscopic silicon seed particles, which are fed from above. In the reaction zone, silane decomposes at 650 °C to 700 °C, while TCS decomposes at 1000 °C.

When the appropriate temperature is reached, the Si is deposited on the seed particles until they grow into larger polysilicon grains that fall to the bottom of the reactor. Grains can be continuously removed from the bottom, in contrast to the Siemens process, which works in batches [30].

FBR technology produces polysilicon in small round spheres (granules). This granulate offers several advantages over conventional polysilicon from Siemens chunks.

- Granulated polysilicon is packaged in flexible bulk containers that reduce handling costs and waste.
- The fluid nature of granulated polysilicon enables the automation of material handling, crucible filling and refill/recharge processes.
- FBR's granulated polysilicon maximises the initial fill weight of the crucible, resulting in a higher yield of ingots during production cycles.

In principle, slightly more energy is consumed for the production of silane, but when considering the entire process, the FBR should save energy for cooling water and energy recovery from waste and exhaust gases in the process compared to the Siemens process. In addition, it is possible to achieve an almost 100% conversion of the silane gas in the reactor in one cycle, whereas the Siemens process can produce 1 tonne of poly-Si and 15–20 tonnes of STC.

One of the disadvantages of the FBR process is the generation of silicon dust that has to be fed back into the process. Dust reduction requires a very careful coordination of temperature and flow rate. FBR is a hot-wall technology. When the silane gas is heated from the outside, it tends to stick to the linings of the reactor walls, resulting in unwanted deposits on the walls and metal contamination of the lining. Therefore, one of the objectives is to prevent Si from coming into contact with the wall cladding.

The question also arises as to how the polysilicon spheres formed can be removed from the reactor. It is possible to suck them out or to drain them at the bottom of the reactor. In both cases, the spheres must pass through a series of philtres, degassers and coolers, where there is a possibility that the surface of the silicon sphere will be contaminated with metallic impurities. The formation of porosity in the spheres and the attraction of oxygen is also possible.

In conclusion, the existing industry is reluctant to use silane gas because it is highly pyrophoric and there are examples of explosions. To summarise, while the Siemens process is still the leader in poly-Si production, the FBR method offers certain opportunities to increase efficiency and profitability. Each method has its advantages and disadvantages, and the choice depends on specific production goals and priorities [28,30]. According to the estimate [31], the Siemens process will retain a mainstream position in the next 10 years, and the fluidised bed reactor (FBR) process will remain the second most important technology for the production of poly-Si. Nevertheless, the market share of the FBR process will increase slightly from 8% in 2022 to 22% in 2033.

### *3.3. Production of Monocrystalline Si*

After the production of SG-Si, the next step is the production of monocrystalline or polycrystalline Si material (ingots), from which thin wafers with a good crystallographic structure are produced, from which solar cells are finally manufactured. Monocrystalline silicon is a material in which the silicon atoms are arranged in a long-range order with a specific orientation. Multicrystalline (polycrystalline) material consists of differently orientated crystals of different sizes.

There are different methods for obtaining single-crystal silicon [32], and the majority of the PV industry uses two methods. The first is the Czochralski (CZ) method, which is based on the pulling process. Another method of zone melting is known as the floating zone (FZ) process [10].

#### 3.3.1. The Czochralski Process

The steps of the Czochralski process include the following [33]:

- Melting: In the first step of the CZ process, high-grade Si feed stocks are melted in silicate crucibles at temperatures above the melting point of Si (above 1414 °C). The crucible and the starting material are in an inert atmosphere (e.g., argon) to avoid contamination.
- Doping: It is possible to dope silicon and convert it into p-type or n-type Si by precisely adding dopant impurity atoms, such as phosphorus or boron, to molten Si.
- Insertion of a seed crystal: A precisely aligned, rod-shaped seed crystal is immersed in molten Si.
- Crystal growth: The rod of the seed crystal is slowly pulled upwards and simultaneously rotated (the average rotation speeds for the seed crystal and the crucible are 2–30 rpm). As it rises, silicon atoms attach to the seed and form a continuous single crystal. Through accurate regulation of temperature gradients, pulling speed and rotation speed, a large, cylindrical single crystal over two metres in length can be produced from the melt.

There is no direct contact between the walls of the crucible and the crystal, which contributes to the formation of unstressed single crystals. In terms of time, the Czochralski process is relatively slow, with crystal growth rates typically in the range of a few millimetres per hour. In this context, research is being conducted into ways to increase the rate of crystal growth. For example, Jeon et al. [34] investigated crystal growth at a fixed pull rate of 1.0 mm/min. They came to the conclusion that the cooling effect has a major influence on the crystal growth rate. A CZ method using a cooling tube was suggested by Dezfoli [35] as a way to boost the crystal growth rate by up to 25%.

Another disadvantage of the CZ method is that for each cycle of crystal growth, a long idle time is required for dismantling and setting up the furnace [25]. For this reason, a semi-continuous or continuous process of crystal growth is considered [32].

It is important to note that although the Czochralski process is widely used due to its ability to produce high-quality crystals, it is also sensitive to impurities that can cause defects in the crystal lattice structure [36]. The quality of the crystals is highly dependent on the melting temperature profile. Therefore, strict control of the process parameters and conditions is crucial for successful crystal growth.

Before the wafers are produced, the ingots are disassembled, and the edge areas are cut off. The monocrystalline cylindrical ingots are disassembled to produce cubic ingots.

The maximum utilisation of the ingot obtained after cutting the seed, the shoulder and the end cone is around 85, without taking remelting into account. The usable mass of the brick is about 58.8% for the M6 and 54.7% for the M12 cell format, considering the geometrical constraints of a square cell from a round ingot [37]. In order to better utilise the mass of the ingot, attempts have been made to grow square silicon ingots [25].

The Czochralski process enables large crystal diameters (46 cm) and masses of up to 1500 kg, and a further increase to 750 mm is expected within the next 10 years [38]. However, the measurement technology and process tools for larger wafers pose a challenge.

The weakness of the Czochralski method is that it can lead to crystal defects such as dislocations and stacking faults. Another drawback is the relatively low homogeneity of the crystal's axial and radial dopant concentration, which results from melt oscillations during crystal formation. This makes it difficult to obtain high-resistance CZ wafers with a specific resistance of over 100 Ohm cm. A magnetic field ("Magnetic Czochralski", MCZ) can delay these oscillations and enhance the homogeneity of the dopants in the ingot [25]. Ongoing research is focussed on refining the Czochralski process to further reduce crystal defects and improve the purity of CZ wafers [39,40].

#### 3.3.2. Float-Zone Process

One end of a polycrystalline Si ingot is brought into contact with a monocrystalline Si seed crystal. From here, a tiny portion of the poly-Si is melted using a Radiofrequency (RF) coil to create monocrystalline silicon from the crystallographic orientation of the seed crystal. The RF coil and the molten region move along the entire ingot. The molten zone contains the impurities because most of them are less soluble in the crystal than in the molten Si. The impurities are concentrated near the end of the crystal, where they can eventually be simply cut away [32]. To further reduce the concentration of residual impurities, this procedure can be carried out once or several times. Doping takes place during crystal growth by introducing doping gases into the inert gas atmosphere, such as phosphine ($PH_3$), arsine ($AsH_3$) or diborane ($B_2H_6$).

The major advantage of the FZ process is the very low content of impurities in the Si crystal [41]. Specifically, compared to CZ silicon, the concentration of carbon and oxygen is substantially lower, although the FZ process also notes the issue of minor contamination from oxidation [42]. FZ wafers have a more even distribution of dopants, which ensures consistent electrical properties across the entire wafer. The FZ process minimises crystal defects, including dislocations and vacancies. This reduction in defects improves the electrical and mechanical properties of the obtained wafers, making them highly desirable for semiconductor manufacturing.

The float zone process is known for its relatively high production costs compared to other methods. The sophisticated equipment and energy-intensive processes used contribute to its high production costs. The FZ process generally has a lower throughput than the CZ process [32], making it less suitable for large-scale production requirements. The float zone process has declined in the industry from 20% in the 1980s to 5% today.

Researchers and manufacturers are exploring hybrid approaches that combine the strengths of the FZ and CZ processes. These efforts aim to capitalise on the purity of FZ wafers while benefiting from the cost efficiency and scalability of CZ production. This hybridisation could potentially bridge the gap between ultra-high purity and the requirements of large-scale production. In any scenario, the wafers' purity will be either less than or equal to the ingot's purity because there is no method for increasing the purity of Si during the ingot's creation.

### *3.4. Wafer Production*

Once the ingot is obtained, it must be processed further to produce wafers.

For this purpose, the wafers must be shaped and cut. The shaping operations consist of two steps. In the first step, the seed and tang ends of the ingot are removed using a circular saw. Before further processing, the ingots are checked for resistivity and orientation. The ingot's surface is ground in the following step to create a uniform diameter along its whole length. The orientation of the surface is normally checked after grinding. After checking the orientation and the resistivity, one or more surfaces are ground along the length of the ingot. After grinding the surface, wafers are cut to a specified thickness. It should be noted that the surface of the cut remains damaged during cutting, and the damaged layers must be removed during further processing of the wafer. The cut wafers are therefore polished to the desired thickness in a lapping machine using aluminium oxide abrasives, which improves the surface parallelism [43].

In the next step, the wafers are chemically etched to remove damaged and contaminated areas. After etching, the surfaces are polished, first with a coarse abrasive polish and then with a chemical mechanical polishing process (CMP) to make them perfectly smooth.

There are several wafering processes, two of which are most commonly used: Diamod Wire Sawing (DWS) and the Diamond Wire-Assisted (DWA) process. The DWA process combines the advantages of DWS and loose abrasive sawing. A diamond-coated wire is used together with an abrasive slurry (polyethylene glycols (PEG) and SiC powder). The wire cuts the silicon while the slurry helps to remove the material. In DWS technology, the wire consists of a steel core with embedded diamond particles coated with metal (usually nickel). DWA minimises scratches and pits on the wafer surface, while DWS enables faster wafer cutting (higher production rates), lower total thickness variation (TTV) and less metal contamination of the wafer surface. The total thickness variation is currently around 10 µm for all wafer sizes and is expected to fall to around 8 µm by 2030 [31].

The predominant wafering process has shifted from DWA to DWS [44,45] although significant cost reductions are possible if PEG is replaced by water-based liquids [27].

In the DWS process, reducing energy consumption without compensating for the roughness of the sawn tile surface is key to achieving an economical and environmentally friendly process. According to Sefene and Chen [46], the optimal combination of sawing parameters is a wire speed of 0.36 m/s, a feed rate of 0.029 mm/min and a wire tension of 7 N, which leads to a reduction in energy consumption, surface roughness and a material removal rate of 8.53%, 2.85% and 4.86%, respectively, compared to the traditional sawing process.

Sawing is also associated with a considerable loss of high-quality Si through the kerf. Reducing the tile thickness and cutting width can increase the number of wafers produced per kilogramme of silicon brick. In addition, the reutilisation of the Si kerf loss is an important development goal that is currently being worked on [47,48]. In the past, a number of kerfless wafering technologies were also developed, but these have since been abandoned because they were not competitive. Figure 1 describes the trend for kerf loss and average As-cut wafer thickness for n-type wafers.

As can be seen from this Figure, about 35% of the silicon is lost as Si-Kerf. A kerf width of 55 µm is standard for DWS in 2023, and the kerf loss is expected to fall to 45 µm by 2030.

In addition to costs, wafer qualities such as thickness variations, roughness, saw damage below the surface and fracture stability also play an important role and must also be improved. Increasing the diamond wire speed increases the productivity of the process but also the probability that the wafer will break [49,50].

Process Improvement Trends

Thinner wafers, lower kerf losses, higher recycling rates and lower costs for consumables will lead to cost savings. Wire diameters will be continuously reduced, and the recycling of Si and diamond wire will increase over the next few years. Higher tool throughput will improve productivity in crystallisation and wafering and increase yields due to lower kerf losses. This will contribute to further cost optimisation. It is expected

that all technologies will achieve an increase in throughput of between 10 and 30% over the next 10 years. New approaches for notch-free wafer production are still being investigated.

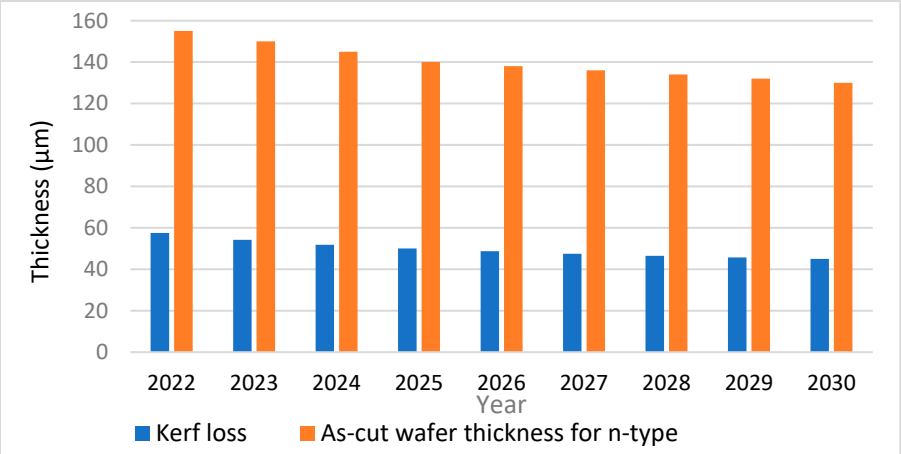


**Figure 1.** Kerf loss in the DWS process and As-cut wafer thickness for n-type wafers (based on data from [31]).

The impact of silicon wafer production on the environment is a growing problem. The process requires the use of chemicals, water and energy-intensive equipment, leading to potential pollution and resource depletion. To mitigate these issues, manufacturers are turning to sustainable practises such as water recycling, energy-efficient manufacturing processes and waste management strategies.

Improvements in wafer surface preparation technology are described in detail in Section 3.6.1.

### *3.5. Power Losses in a Solar Cell*

After the production of wafers comes perhaps the most important activity, namely the production of solar cells and modules. The technology for manufacturing solar cells has developed rapidly since the 1950s, when Bell Laboratories developed the first practical solar cell made of Si with an efficiency of around 4%. Various production technologies have been developed, all with the main aim of increasing the efficiency of the cell and reducing production costs. Increasing the efficiency of the cell means reducing losses. Therefore, it is essential to understand the losses that affect the efficiency of a Si-based PV cell (Table 1) before we discuss the key differentiators of PV cell technology and system performance. More information on losses related to PV cells was given by Oni et al. [51].

**Table 1.** Si-based PV cell losses.

| Optical | Electrical | Degradation |
| --- | --- | --- |
| • Losses due to incomplete absorption of incident light by the cell<br>• Reflection instead of absorption<br>• Because part of the surface is covered by metal contacts, light cannot reach it<br>• Because every material only absorbs a certain range of light wavelengths, some of the incident solar radiation is not absorbed<br>• Absorption in anti-reflexive coatings<br>• Non-ideal light trapping | • Losses caused by hindrances to the cell's current flow<br>• Resistive losses resulting from every material's intrinsic electrical resistance<br>• Energy lost in the form of heat as a result of electron–hole pair recombination<br>• Power losses due to increased cell temperatures<br>• Front surface and emitter recombination<br>• Contact resistance electrode–semiconductor<br>• Loss due to crystal defects | • Losses generated when the cell is subjected to field conditions<br>• Light-induced cell deterioration, which is substantial for p-type silicon wafers doped with boron compounds, occurs within the first few hours of exposure to sunlight<br>• Degradation caused by external factors such as high temperature and humidity |

#### 3.5.1. Optical Losses

Optical losses affect the performance of the PV cell mainly by reducing the short-circuit current. They refer to light that does not produce an electron–hole pair due to reflection at the front surface, absorption in the anti-reflection layers, non-ideal light trapping or because it is not absorbed by the solar cell even though it would ideally produce an electron–hole pair [52].

The front surface of a solar cell is always textured or roughened to increase the probability that light reflected from one inclined surface to another will be coupled into the cell for absorption. The effective path length of light within the cell for absorption and photogeneration is further increased by refraction at an inclined surface. Light trapping at the Lambertian limit can be achieved in Si cells if the back surface is reflective and the front and back surfaces are pyramidal [53].

As the visible spectrum (350–780 nm) contains enough energy to generate electron–hole pairs in the most commonly used semiconductor solar cells, ideally, radiation of the entire visible spectrum would be absorbed. Optical losses can be reduced in various ways.

- The coverage of the cell surface by the top contact should be minimised (although this can lead to increased series resistance).
- Surface texturing and anti-reflective coatings can reduce reflection.
- Surface texturing and light trapping can be applied together to extend the optical path length in the PV cell and boost absorption.

#### 3.5.2. Electrical Losses

PV cells consist of different layers. When the current flows through these layers, it encounters resistance, which we usually refer to as ohmic losses. This resistance is mainly due to the volume resistance of the semiconductor material and the contact resistance at the metal–semiconductor interface. The main resistance is caused by the movement of charge carriers (electrons and holes) through the silicon crystal lattice. Imperfections, impurities and crystal defects contribute to this resistance. Contact resistance occurs at the points where metal electrodes are connected to the semiconductor. Ohmic losses lead to voltage drops in the cell and reduce the overall performance. Higher resistance leads to a lower fill factor (FF) and lower efficiency.

There are strategies that can reduce these losses. For example, increasing the thickness of busbars and grid lines on the surface of the cell reduces contact resistance, and using materials with lower contact resistance (such as silver or copper) improves electrical connectivity. Optimising the doping profile within the semiconductor layer can minimise volume resistance.

New, advanced cell concepts, such as PERC (Passivated Emitter Rear Contact), aim to reduce resistance and increase cell efficiency.

Whilst reducing resistance is important, other factors (e.g., light absorption, carrier lifetime and recombination losses) must also be considered. Thicker conductors block more sunlight, which affects absorption. In addition, aggressively reducing losses can increase the complexity and cost of manufacturing. To summarise, understanding and managing resistive losses is key to improving PV cell efficiency.

#### 3.5.3. Recombination Losses

The process in which the charge carrier electrons and holes combine and neutralise each other is known as recombination. This takes place within the semiconductor material of a PV cell. Recombination affects both the short-circuit current and the forward injection current (which affects open-circuit voltage). When recombination occurs, fewer charge carriers contribute to the current, resulting in lower current consumption.

Recombination occurs at the cell surface, where the charge carriers recombine before they reach the contacts (surface recombination), but also in the bulk of the semiconductor material (bulk recombination) and in the depleted region near the p–n junction.

There are different types of recombination. In radiative recombination, the electrons lose energy and recombine with holes, emitting photons (light). This type is less important for silicon-based solar cells. Another type of recombination occurs due to defects or impurities in the material that lead to the recombination of charge carriers. The third type is Auger recombination. Auger recombination is a three-particle process that is more important at high charge carrier concentrations. During this process, a hole in the valence band and an electron in the conduction band recombine, but the excited electron does not emit photon energy. An excited electron in the conduction band transfers its energy to another electron in this band. The second electron rises to a higher energy level with the additional energy, as it now has greater kinetic energy. After a certain time, the electron returns from the higher energy levels to the edge of the conduction band. The valence band is another place where the same scenario can occur. As the opposite of the last scenario, where two electrons and one hole were involved, two holes and one electron are needed in this case. High recombination increases the forward diffusion current, which decreases the open-circuit voltage. In summary, minimising recombination losses is crucial for optimising PV cell performance and maximising energy production.

When solar cells work, they inevitably generate heat. Heat can be generated by various processes, e.g., absorbed sunlight, resistance losses in the electrical contacts of the cell and even environmental factors [54]. The influence of temperature on the performance of solar cells is complex and can have both positive and negative effects.

The efficiency of photovoltaic (PV) cells decreases with increasing temperature, which is due to the intrinsic physical properties of the semiconductors used in the cell. As the temperature rises, the kinetic energy of the charge carriers (electrons and holes) within the PV cell increases. Higher kinetic energy leads to more random movement of the charge carriers, which affects their ability to contribute to the cell's electric current [54].

The voltage generated by a PV cell is directly related to the energy difference between the valence band and the conduction band. Higher temperatures lead to a shift in the energy levels, which reduces this energy difference. As a result, the open-circuit voltage decreases, which affects the efficiency of the cell. At the same time, the short-circuit current can increase slightly due to increased charge carrier mobility. The efficiency of a PV cell is determined by the trade-off between an increase in the short-circuit current and a drop in the open-circuit voltage. Unfortunately, the decrease in voltage predominates, which leads to a decrease in overall efficiency with increasing temperature [55].

For the reasons mentioned above, it is desirable for the solar cell to have a lower temperature, which can be achieved by improving heat dissipation to the environment (passive method). The thermal emissivity of Si-based PV cells plays a role in the operating temperature of the solar cell. Encapsulated and non-encapsulated c-Si solar cells are good emitters of radiation but with different effects [56]. The emissivity of the non-encapsulated c-Si solar cell was determined to be 75% in the MIR range, and the emission of free charge carriers dominates in the highly doped emitter and back surface layers of the array. Both effects are enhanced by the improved optical connectivity resulting from the texture of the front surface. The glass-covered encapsulated cell has an average emissivity of about 90% in the MIR range, which drops to 70% at 10 μm wavelength and is dominated by the emissivity of the cover glass. These results indicate the possibility of optimising the emissivity of c-Si based collectors and thus the cooling of the cells [57].

#### 3.5.4. Losses Due to Degradation

A lesser-known phenomenon that affects a large part of the crystalline silicon cell market is light-induced degradation (LID). In simple terms, this is the deterioration of solar cells due to solar radiation in the first few days after installation. This may result in 0.5% to 1.5% in losses.

The development of boron–oxygen compounds in the silicon wafers that constitute the solar cell is usually the cause of LID. This indicates that the highest LID occurs in

boron-containing monocrystalline p-type solar cells. LID also occurs in multicrystalline p-type cells but is less pronounced due to lower oxygen content.

In n-type silicon, no LID occurs because the material does not contain boron. In this case, the LID loss should be set to 0% instead of the default value.

Thermal expansion and contraction, UV light and damage from wind-blown particles also reduce cell performance over time.

The degradation of PV cells is the progressive deterioration of their physical properties, which leads to a decrease in output power over the years. The type of PV technology used and the environment in which the PV modules are installed determine their ageing. The main external factors that influence degradation are temperature, humidity, UV radiation, dust accumulation, irradiance and wind speed. The ageing of the PV cell and the different types of degradation have different effects on the electrical properties of the cell [58].

The most important types of degradation described in the literature are cracking, discolouration, delamination, corrosion, hot spots and blisters. As moisture can penetrate the cell housing, installing PV panels in hot, humid locations increases the likelihood of this type of failure. The components are damaged by the chemical reaction of the moisture with them. The primary effects of delamination are related to the optical decoupling of the materials. As a consequence, reflection of the incident light increases, which leads to a decrease in transmission. Moisture ingress causes the PV module to corrode, impairing the adhesion of the individual cells to the metal frame of the module and weakening the metallic connections between the cells. This leads to an increase in leakage currents and, finally, to a decrease in efficiency [58].

### *3.6. The Technological Steps Involved in the Production of the PV Cells*

After understanding the losses associated with the efficiency of PV cells, the technological steps involved in the production of the cells and ways to reduce certain losses at each step are considered. Although different types of PV cells have been developed and are available on the market, they all have some manufacturing steps in common [59].

1. Surface preparation;
2. Emitter formation;
3. Edge isolation;
4. Cleaning;
5. Passivation;
6. Anti-reflective coatings;
7. Front contact formation;
8. Back contact formation;
9. Co-firing.

#### 3.6.1. Surface Preparation

Surface preparation serves two purposes—firstly, to remove damage caused by cutting the wafer and, secondly, to reduce the reflection of the board surface by giving it a matt colour. This is usually achieved with wet benches, although a dry etching solution is also available. This process, called texturing, is the centrepiece of surface preparation. Wet chemical tools are also used to clean the cells to remove unwanted side effects of the diffusion process. This refers to the removal of phosphorus silicate glass (PSG) in PERCs and borosilicate glass (BSG) in TOPCon, as well as edge isolation to remove the emitter that forms on the edges of the wafer, as well as on the other side. Wet benches are also used to polish the backs of the cells, a step that is often integrated into edge isolation tools.

For most equipment suppliers, TOPCon has become the reference point for every product's improvement. A hot topic in this context is the optimisation of the texturing process to achieve a reflectance of less than 9% with new additives developed exclusively for TOPCon. Although not explicitly mentioned, surface cleaning is becoming increasingly important in TOPCon and SHJs compared to PERCs. There are three process routes for surface cleaning: standard cleaning (known as RCA) (hydrogen peroxide + ammoniacal

nitrogen), hydrogen peroxide ozone cleaning and pure ozone cleaning. A one-minute process time and a good cleaning effect at room temperature are made possible by ozone-based cleaning. In addition, ozone-based cleaning enables controlled etch-back of the emitter in PERC-based PV cells and rounding of the pyramid tips of textured surfaces, which is preferable for silicon heterojunction (SHJ) PV cells. Ozone-based cleaning can increase production throughput and is, therefore, currently the most commonly used method [60,61].

The aim of the texturising process is to create a surface that reduces light reflection. This is achieved by using alkaline solutions suitable for monocrystalline wafers (acidic solutions are suitable for poly-Si). While SDE (Saw Damage Etching) is an aggressive solution for removing the outer silicon layer, texturing requires very controlled etching.

Many researchers have investigated the problem of light trapping by structured surfaces. In their work, McIntos et al. [62] propose the use of a parameterisation of light trapping in wafer-based solar cells to predict the absorption of a solar cell as a function of wavelength and cell thickness, from which the generated current can be calculated for each incident spectrum. The experimental investigation of light trapping in isotextured wafers is presented in a paper [63]. Their results show that the light trapping in isotextured wafers is only weakly dependent on the etch time of the isotexture.

Cost reductions in PERC technology are achieved by eliminating SDE prior to texturing and reducing chemical consumption. In TOPCon technology, no or very little SDE is applied, and KOH consumption is significantly reduced.

PERCs use texturing in the form of classic pyramids, where there is still room for optimisation in terms of pyramid arrangement and reducing the consumption of chemicals, especially KOH. The ultimate goal of texturing with PERCs is to reduce the reflectance below 10% at a light wavelength of 600 nm.

TOPCon technology applies a customised texturing process with a specially developed additive that results in a different pyramid shape than PERCs. The optimal size of the pyramid is approximately 1 µm, and the arrangement of the texture is continuously optimised [60]. The aim is to achieve a reflectance of less than 9% at 600 nm.

In their study, Huo et al. [64] demonstrate the use of a sodium hydroxide (NaOH) solution with a cheap additive (ethylene glycol butyl ether) to etch and prepare inverted pyramidal structures on mono-Si surfaces. The method is simple, cheap and fast, causes no precious metal pollution and is particularly compatible with today's industrial production lines for Si PV cells. According to their research results, the inverted pyramidal structures show less reflection than conventional upright pyramidal structures and flat polished silicon plates.

In their second paper, Mcintosh et al. [65] investigated light trapping in Si wafers textured with conventional random pyramids on the front side and rounded random pyramids on the back side, as it was found that the rounding of the pyramids led to better surface passivation. They concluded that the current generated was approximately constant for etch durations of less than ~60 s and decreased significantly with increasing etch duration. Thus, by limiting the duration of the rounding etch, better surface passivation can be achieved without deterioration in light trapping.

Schmid developed an advanced texturising solution that also uses an alkaline solution. The process enables one-sided precision processing of the front side, while the reverse side remains completely unchanged. The company has patented a pressure-free spray system that applies a hot solution to the surface to create a pyramid-shaped texture. The process sequence is pre-cleaning, alkaline texturising with a KOH bath at elevated temperatures, followed by rinsing, metal and ozone cleaning and finally rinsing and drying. The process takes place at 60 to 80 °C, depending on the additive. An important feature of the technology is the reduction in water consumption by around 30%, with typically 4 to 5 µm of silicon being etched from the surface. This achieves a light reflection value of less than 12% at 400 to 1000 nm and less than 9% at 600 nm. At the same time, the process leads to good uniformity of results not only within a single tile but also between series of wafers [60].

Liu et al. [66] propose a traditional wet acid etching system with incorporated manganese dioxide ($MnO_2$) particles in order to improve the texturing performance of mc-Si wafers.

#### 3.6.2. Emitter Formation

Diffusion is the step that follows the process of surface conditioning. Physically, a solar cell is essentially a p–n junction diode. To realise a solar cell from input wafers, the emitter is formed by doping a silicon substrate with the opposite polarity to the base. PERCs, which are based on a p-type wafer, therefore require phosphorus diffusion, while TOPCon cells, which are usually based on an n-type wafer, use boron diffusion to create an emitter.

Diffusion furnaces are used to produce emitters. Although the dopant can also be introduced by zone implantation, thermal furnaces are still required to activate the dopant. At the same time, the leading manufacturers of TOPCon have already started work on laser-selective emitters.

However, in order to facilitate the production of layer-resistant emitters and to fully exploit the development of metallisation pastes, low-pressure diffusion is being used, which took on the role of a cutting-edge technology a few years ago.

With TOPCon technology, diffusion takes place at temperatures above 1000 °C and requires longer cycle times, resulting in a lower flow rate. Boron precursors of choice can be boron tribromide or boron trichloride ($BCl_3$). Boron tribromide has been the standard in the past. However, it has a side effect; a by-product of the process acts like an adhesive for quartz, which can shorten the operating time. Some equipment manufacturers have significantly optimised the process, while others have switched to boron trichloride ($BCl_3$), which is easily removed from the surface and has become widely accepted. The disadvantage of using boron trichloride is its corrosive nature and associated safety issues.

It is possible to deposit the amorphous silicon-based layer (also known as the a-Si doped layer) by low-pressure chemical vapour deposition (LPCVD) [67,68], plasma-enhanced chemical vapour deposition (PECVD) [69–71] or by spraying [72]. PECVD is frequently used in industry for the deposition of $Al_2O_3$. It is usually considered a one-sided deposition technique, although minimal deposition can occur at the cell edges, which can be removed by online wet chemical etching. However, a challenge with PECVD is the risk of bubble formation due to the large amounts of hydrogen embedded in the Si layer, which places limits on the maximum layer thickness [73]). Currently, LPCVD is the most advanced technology in the photovoltaic industry for the deposition of a-Si or poly-Si layers [60]. The numerous advantages of this method include high layer homogeneity, satisfactory step coverage, high repeatability and the possibility of creating the required interfacial oxide layer in situ. The disadvantages of this technique include an inherent double-sided deposition (wrapping), its relatively low deposition rates and the formation of doped glass. Double-sided deposition can lead to a deterioration of the optical and electrical properties of the cells, such as open-circuit voltage, short-circuit current density and fill factor [59,74]. Therefore, additional processing steps are always required for cladding and edge shunts, such as stripping the cladding by masking and/or stripping the cladding layer on one side, followed by edge isolation by dry etching or chemical etching or laser cutting.

In PERCs, the glass is removed with diluted Hydrofluoric Acid (HF), and the backside is doped by light etching. These two steps are carried out in a single pass, usually inline with HF and $HNO_3$. Acidic solutions are generally used for this application, but the use of alkaline chemicals is also in vogue. Dry etching is an alternative to wet chemical solutions for the removal of coatings.

#### 3.6.3. Edge Isolation and Cleaning

Edge isolation usually starts with one-sided oxide removal with HF, and the backside is polished in a KOH bath at elevated temperature. While the back is being etched, the front is protected by a water masking technique. This is followed by rinsing and cleaning of the surface.

#### 3.6.4. Passivation

The passivation of PV cells is an important process that helps to increase the efficiency of PV cells. On the wafer's surface, dielectric layers are placed. Most silicon wafers cannot be completely free of impurities or crystal lattice defects on both surfaces that act as recombination centres. Passivation is a process that deactivates these defects and reduces the surface recombination of charge carriers, thereby maintaining the efficiency of the cells [75].

Excellent surface passivation on the front and back of the PV cell is essential to achieve higher efficiency on c-Si substrates [76]. PV cells with poly-Si-based passivating compounds on both the front and back of the cell may be able to achieve efficiencies of more than 26% [77].

The basic technology that could bring c-Si-based PV cells closer to the theoretical efficiency limit is carrier-selected contacts (CSCs). The passivated tunnel oxide contact (TOPCon), which is very different from the current standard heterojunction solar cells, is a novel and groundbreaking method in this field. Its main function is to reduce the recombination of minority carriers at the interface [78].

The tunnel oxide can be deposited thermally or as part of another deposition method used to deposit polysilicon, the centrepiece of the TOPCon process. Almost every deposition technology used in photovoltaics is promoted here—LPCVD, PECVD, APCVD, ALD and PVD—although LPCVD and PECVD are the mainstays today.

Based on the PERC idea, one possible technology is the phosphorus-doped electron-selective contact (n-TOPCon). Very high efficiency (>25) has been achieved by the passivated contact approach in c-Si solar cells fabricated with SiO2 and polycrystalline Si.

One important component of TOPCon solar cells is the poly-Si layer that is deposited on the rear side. The processes of LPCVD or PECVD are typically used to produce the TOPCon layer, which comprises tunnel oxide and doped poly-Si and is necessary for charge carrier selectivity [79]. In the industry today, LPCVD n-doped poly-Si layers are still the mainstream, usually in combination with ex situ doping, i.e., n-doping of the intrinsic Si layer in a subsequent POCl3 diffusion process. The ITRPV 2022 roadmap shows that the transition from the LPCVD to the PECVD process will happen in the coming years [31]. As the deposition rate for in situ doping in this method is the same as for intrinsic poly-Si, PECVD TOPCon layers are usually doped during deposition. At Fraunhofer ISE, in situ phosphorus-doped LPCVD layers became the basis for the industrial approach of TOPCon technology [80].

#### 3.6.5. Anti-Reflective Coatings

Solar cells must have a high absorption coefficient and low reflectance in the visible to near-infrared spectrum in order to work efficiently. Anti-reflective coating (ARC) is used in PV cells to improve light absorption and reduce reflection losses, thus improving the energy conversion efficiency of solar cells. In addition, ARC should fulfil various other requirements, such as abrasion resistance, chemical thinning and moisture-induced degradation [81]. This is a rapidly evolving field with continuous research and development. The latest trends in the application of anti-reflective (AR) coatings on crystalline silicon (c-Si) cells include the following [82–84]:

- Thin-film AR coatings: Current research is mainly focused on multilayer AR coatings.
- Gradient refractive index structure (GRIN): Adhesion and permeability efficiency are significantly increased by the GRIN structure, which virtually eliminates contact between the cells.
- High–low–high–low refractive index (HLHL) structure: The HLHL structure achieves considerable AR efficiency with fewer materials, while the selection of materials with opposite stress properties facilitates stress management. However, more advanced methods are needed to create these two structures.

- Embedding of nanoparticles: There is also a trend towards embedding nanoparticles in the AR layer. For example, the efficiency of cells with a $SiO_2$ AR coating and indium nanoparticles (In-NPs) embedded in the $SiO_2$ layer has increased significantly.

There are currently two main strategies for achieving the anti-reflective effect. Firstly, thin layers such as single-, double- and multilayer coatings are applied to the substrate, and secondly, GRIN coatings with porous and nanostructured arrangements such as moth-eye structures are used [85].

The thin-film coating reduces the reflection that occurs at different layers due to the principle of destructive interference. This increases the amount of light absorbed by the cell and converted into electricity. The ARC consists of a thin layer of dielectric material. Various materials such as aluminium oxide ($Al_2O_3$), silicon dioxide ($SiO_2$), titanium dioxide ($TiO_2$), magnesium fluoride ($MgF_2$), silicon nitride ($Si_3N_4$) and zinc oxide (ZnO) have been used as AR layers [86–88]. The ARC's thickness is selected so that the dielectric material's wavelength is 25% of the incoming wave's wavelength. The reflection is further minimised if the refractive index of the anti-reflection layer corresponds to the geometric mean value of the materials on both sides, i.e., glass or air and the semiconductor.

The latest generation of single-layer ARC, known as GRIN coatings, overcomes limitations such as ARC effectiveness within a limited wavelength range and at normal light incidence. Various profiles of gradient refractive index layers have been proposed for omnidirectional and broadband ARC, including linear, parabolic, cubic, quintic, Gaussian, exponential, exponential–sinusoidal and Klopfenstein [85]. Linear index profiles can be easily achieved on silicon substrates. In one study, SiNx films with a linear index profile were described as an anti-reflective coating with low reflection in the near-infrared range and in the visible range for a large angle of incidence.

#### 3.6.6. Front and Back Contact Formation

Technically, a silicon wafer is a solar cell when the p–n junction is formed, but it only becomes functional after metallisation. The metal contacts play a key role in the production of highly efficient and cost-effective crystalline Si PV cells. For both polarities, electrons and holes, the metal contacts must conduct charge carriers at low ohmic contact resistance to the corresponding silicon surfaces [89]. This step also lays the foundation for the serial connection of cells in modules via buses.

The metal contacts are usually designed as a so-called finger grid, which consists of several conductors in order to transport the photogenerated current to busbars with low resistance losses. To connect the solar cells in the module, the metal contacts on the busbars must ensure a reliable electrical solder connection to the strips or wires. The metal contacts should only cover a small portion of the Si wafer to minimise shading losses from incident sunlight and to reduce the recombination of minority charge carriers on the metal surface. The choice of metallisation technique is closely linked to the interconnection scheme used in module fabrication and vice versa; this consequently affects the design of the metallisation grid. A key parameter of the grid design is the finger length, which is defined here as the maximum distance the current must flow along the finger (i.e., half the distance from busbar to busbar in a standard H-pattern).

For decades, screen-printed Ag front and Al back metal contacts have been used in most industrial solar cells [90]. Ag forms a good electrical contact to n-type silicon and Al to p-type silicon, which is an advantage of this technique. Additionally, the screen printing process allows for a very low cost and high throughput patterned deposition of the µm wide metal finger grid with excellent conductivity. For this reason, screen printing technology still has a market share of more than 85% [91]. Lower consumption of Ag paste and cheap, high-throughput screen printers have helped to reduce the production cost of a PV module from approximately USD 5/Wp in 2000 to less than USD 0.25/Wp in 2020. In order to attain material sustainability, the PV industry must reduce Ag consumption per PV cell from 20 mg/W in 2019 to less than 5 mg/W in 2028, according to recent projections [92].

This can be accomplished by using different printing methods or by using Cu and Al pastes in place of traditional Ag pastes [93,94].

The industry returned to standard 11 µm wire screens, and the 430-mesh screen was mainstream in 2022. These screens support finger openings of 20 or 21 µm, which is the current state of the art for PERCs [95]. Cell manufacturers can reduce the finger width to a range of 23 to 25 µm, with a few even reaching 20 µm [60].

TOPCon has silver on both sides, so the silver consumption is twice as high. This is not a problem as long as TOPCon production is up to 100 GW. At much larger capacities, silver becomes a problem, which is why the industry is looking for alternative solutions, such as the partial or complete replacement of silver with aluminium, at least on one side [92]. Other solutions use copper, whereby the silver layer is printed first and then the copper is applied on top. High-temperature copper pastes suitable for TOPCon metallisation are also being investigated. However, all of these approaches are still in the research and development phase [60], including laser-enhanced contact firing [96].

The pastes can now be stored at room temperature or in a standard refrigerator, which greatly simplifies storage and shipping and results in significant cost savings. Curing can now be performed much faster and with an infrared oven, reducing both the heat budget of the cell and the space required by the oven in the production environment. Certain pastes now reach their optimum volume stability after just a few minutes at only 150 °C.

The industry is not only working on pastes but also on alternative metallisation processes such as dispensing and rotary printing, which come very close to screen printing, smart wire contacting technology, pattern transfer printing, inkjet/flextrail printing and also plating [97]. Plating is an alternative technology that has been around for some time but has not yet achieved commercial success.

### *3.7. PV Cell Technologies*

The most popular PV cell technologies in use today are PERCs, TOPCon, IBCs, HJTs, Multi Busbar cells, half-cut and 1/3 cut cells, Shingled Cells, Gapless Cells and Bifacial solar cells.

#### 3.7.1. PERC Technology

PERCs, a modern, fundamental technology, are used to overcome the disadvantages of conventional solar cells with an aluminium back-surface field (Al-BSF). One of the main features of PERC technology is the use of a passivation layer on the back of the cell that reduces electron recombination and thus enhances the efficiency of the cell. The passivated layer between the solar cells and the encapsulation material prevents photons from hitting the backsheet. This in turn keeps the temperature of the backsheet low, which enables higher power output from the PV panel [98].

This technology also includes a reflective layer that bounces light back through the cell, allowing it to absorb more energy. In addition, PERCs perform better in low-light conditions and have a higher overall efficiency than conventional solar cells. The disadvantage of PERC solar modules is their sensitivity to shadows.

#### 3.7.2. TOPCon PV Cells

TOPCon stands for Tunnel Oxide Passivated Contact and is a more advanced N-type Si cell architecture that offers several advantages over PERC architecture. Fraunhofer ISE, a German solar research organisation, first proposed the TOPCon concept in 2013, but large-scale implementation of the technology was not achievable until 2019. The front side of the TOPCon cell and the structure of a conventional N-type solar cell are identical. The main difference is the back of the cell, which has a layer of ultra-thin silicon oxide and a thin layer of doped silicon.

The basic idea of the TOPCon concept is that the metal of the connection contacts does not come into contact with the silicon layer. TOPCon technology solves this problem by using a thin layer of insulating material (a tunnelling oxide layer) between the metal

contact and the solar cell (Figure 2). This layer creates a tunnelling junction that enables better electron transport and collection, resulting in higher cell efficiencies. Thanks to the passivation of the cell surface with a thin layer of silicon oxide, the recombination rate of electrons is also reduced. TOPCon solar modules therefore also work better in low light. This makes them ideal for use in areas with less sunlight, e.g., in cloudy or shady regions.

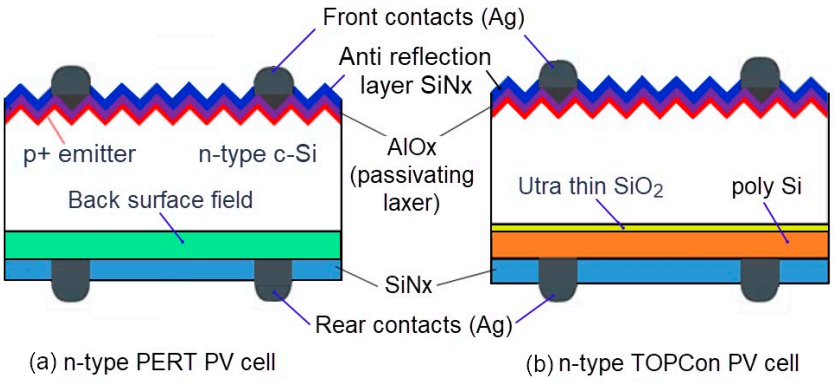


**Figure 2.** A standard PERC cell (**a**) and TOPCon cell (**b**).

The thin oxide layer also protects the cell from extreme environmental influences such as humidity and temperature fluctuations, which can normally lead to cell degradation. This means that the technology ensures a longer lifespan for the cells, as they are less susceptible to degradation over time. TOPcon can be integrated into existing PERC lines with relatively low investment, which is a major advantage. Despite these advantages, in addition to more complex production and increased sensitivity to impurities, a very important challenge of TOPCon technology is the increased use of silver, which increases production costs. For this reason, ongoing research and development work is focused on reducing the silver content in the cells without compromising efficiency and enhancing the reliability of TOPCon technology [92].

#### 3.7.3. IBC Cell Technology

Interdigitated Back Contact (IBC) solar cells are a sophisticated technology that enhances the efficiency of PV modules. One of the key features of IBC technology is the rearrangement of solar cell components to reduce power losses and increase cell efficiency. This is achieved by moving the electrical contacts to the back of the cell, minimising shading on the cell surface and allowing for greater light absorption [99]. The cells usually use a crystalline silicon (c-Si) wafer, with monocrystalline silicon being favoured due to its higher efficiency. An anti-reflective and passivation layer, often made of silicon dioxide, is applied to one side of the c-Si wafer to further improve light absorption and reduce losses. The interdigitated layers of n+ and p+ emitters in the diffusion layer are critical to the operation of the cell as they enable the separation and collection of electron–hole pairs. It is also possible to combine IBCs with other technologies (TOPCon or HJTs) [100].

Despite their higher efficiency, IBCs are more complex and expensive to manufacture compared to conventional Al-BSF cells. However, their lower series resistance and the decoupling of optical and electrical optimisation make them a valuable choice for high-efficiency solar applications [101]. As the back layers support the entire cell and prevent microcracks that can ultimately lead to failure, IBC silicon cells are not only more effective than conventional cells but also more stable.

#### 3.7.4. Heterojunction—HJT Cells

Heterojunction PV cells (HJT) use a base of ordinary crystalline Si with additional ultra-thin layers of amorphous Si on both sides, forming a so-called heterojunction. The additional amorphous silicon layers reduce the recombination at the n–p junction, which means that they reduce losses and increase cell efficiency [102]. The HJT cells' exceptionally

low temperature coefficient, which is about 40% lower than that of traditional crystalline multi- and mono-silicon cells, is their most impressive attribute. This is a particular advantage in hot climates but also in general with regard to general climate changes that lead to more and more hot days [103].

A comparison of the power temperature coefficient is listed as follows:

- Poly-Si, P-type cells 0.40 to 0.43%/°C
- Mono-Si, PERCs 0.35 to 0.40%/°C
- Mono-Si, TOPcon 0.30 to 0.34%/°C
- Mono-Si, IBCs 0.27 to 0.31%/°C
- Mono-Si, HJTs 0.25 to 0.27%/°C

In addition, the use of indium tin oxide (ITO) or other transparent conductive oxides in HJT cells improves their conductivity and reflective properties. These cells have achieved impressive efficiencies, with monofacial HJT solar cells reaching up to 26.7%. In addition, due to their symmetrical structure, HJT modules often have a bifaciality factor of over 90%, allowing them to capture sunlight from both sides and further increase energy yield. As a general overview of the technologies described above, it can be said that there is still a need for research in the development of passivating high-temperature contacts with a selective surface on both sides of the PV cell ("advanced TOPCon"), in the improvement of the transparency and conductivity of HJT contacts ("advanced HJT") and in the combination of the latest HJT or TOPCon technologies with an IBC structure.

The market for solar modules has evolved in recent years, moving away from the relatively exclusive, ribbon-based connection of full-square solar cells to a range of cell formats and connection technologies that are constantly improving performance (e.g., split cells, shingled cells, high-density cell interconnection).

#### 3.7.5. Multi-Busbars Technology

Of the many cell improvements, multi-busbars (MBBs) are the most commonly used technology to increase efficiency. Traditional ribbon busbars (5BB or 6BB) are rapidly being replaced with nine or more thin wire busbars (9BB or 12BB). Some manufacturers have even switched to 16 micro-wire busbars. Wider cells also allow more busbars to fit on the cell surface. Up to 18 or 21 busbars can be integrated into 210 mm cells.

#### 3.7.6. Split Cells

In recent years, most leading manufacturers have switched to using half-size cells instead of the full-size square cells (Figure 3). After the square cells have been split in half by a laser, they are joined together to form the upper and lower cell groups, which work in parallel.

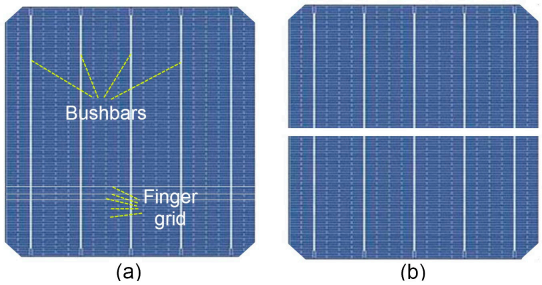


**Figure 3.** Full size cell (**a**) and half-cut cell (**b**) (three fingers are highlighted in the picture on the left).

This cell design has several advantages because each group of cells operates at the same voltage but at half the current. Since the electrical losses are proportional to the square of the current, they are significantly lower in this case, which results in less heating of the module and its higher efficiency. The halved current not only lowers the operating temperature of the cells but also reduces the intensity of hot spots caused by localised

shading, dirt build-up or cell damage, providing extra durability and reliability. As each group of cells is only half the size, the distance between the busbars is also halved, allowing smaller busbars to be used, resulting in lower shading losses on the busbars and higher efficiency. Compared to full solar cells, half-cut cells provide 2–4% more power. The most important advantage of split-cell technology is at partial shading of the surface. If one part of the PV module is shaded, this has no effect on the performance of the unshaded part. This is a result of the two cell sections acting as two separate, tiny modules since they are connected in parallel [104]. A primary drawback of half-cut solar panels is its slightly higher price (0.6 to 1.2%). Recently, some manufacturers have started to produce particularly large square cells of 210 mm that can be cut into three parts (1/3 cut). This enables a low-current module with a higher system voltage, allowing the inverter to start earlier and achieving higher power generation capacity.

#### 3.7.7. Shingled Cells

Shingled cells is a new approach that uses overlapping thin cell strips assembled horizontally or vertically across the panel (Figure 4). A typical full-size cell is laser cut into five or six strips. The resulting strips are then overlapped and glued on the back using an electrically conductive adhesive (ECA) to form long narrow strips with 34 to 40 cells in a string, depending on the size of the panel. Usually, the overlap is from 1 to 2 mm.

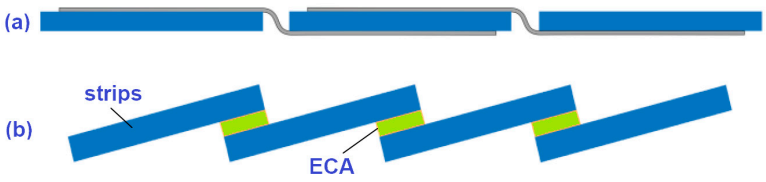


**Figure 4.** Cell interconnection: conventional ribbon (**a**) and shingle (**b**).

This design covers a larger area of the panel (matrix shingling) as it does not require busbar connections on the front (higher power per square metre). Shingled solar modules eliminate the busbars that connect the individual cells together, reducing the power losses associated with degradation at the module level. Another advantage is the fact that long shingled cells are usually connected in parallel (in conventional solar modules, the PV cells are connected in series), which significantly mitigates the effects of shading, as each long cell operates autonomously [105]. Another interesting development in the aesthetics of shingles is the introduction of flexible and curved panels. These panels can be moulded to fit curved or irregular surfaces such as domes or round roofs. The disadvantage of shingle technology is the approx. 2–8% higher silicon consumption due to the overlapping areas and the additional process step required for cell separation and edge passivation.

#### 3.7.8. High-Density Cell Interconnection

To further increase the efficiency of the panel, an idea was produced to reduce the vertical gap between the cells (Figure 5). Conventional large ribbon busbars required a few millimetres of gap to bend between the front and back of the cell. By applying much smaller wire multi-busbars, the gap between the cells can be considerably reduced from around 2 mm to 0.5 mm, as some space is still needed to connect the busbars. As a result, more power per square metre of the PV module can be achieved.

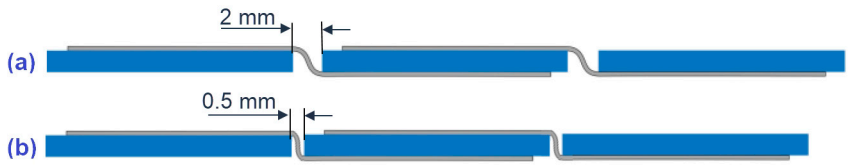


**Figure 5.** Scheme of cell gaps: (**a**) traditional module and (**b**) high-density module.

#### 3.7.9. Bifacial Solar Cells

Bifacial photovoltaic (PV) cells are a significant advance in solar technology, as they can capture sunlight from both sides of the panel. Unlike conventional monofacial solar cells, which only capture the light on the front side, bifacial cells can also utilise the albedo radiation reflected from surfaces such as roofs or the ground [106]. This double-sided capability enables higher energy production, as both the front and the back can generate electrical energy. The efficiency of bifacial cells is measured separately for each side, and the bifaciality factor is defined as the ratio between the efficiency on the rear side and the efficiency on the front side under the same irradiation conditions. Bifacial PV cell technology is not only innovative but also versatile. It is used in various sectors, including agriculture and aquavoltaics, where it contributes to dual land use for energy and food production or is installed over bodies of water [107,108].

#### 3.7.10. Larger Sizes of Solar Cells and Modules

In order to reduce production costs and increase efficiency, most manufacturers have moved from the standard 156 mm wafer size to larger wafer sizes. Although a range of cell sizes are under development, some sizes have emerged as the new industry standard; these include 166 mm, 182 mm and 210 mm.

The industry standard module size of the last decade (2.0 m × 1.0 m) was based on a square cell format of 156 mm × 156 mm with 72 cells. The new modules coming onto the market are up to 2.4 metres long and 1.3 metres wide and are based on 180 and 210 mm cells. This is an increase in size of 20 to 30% compared to conventional panels, which is accompanied by a significant increase in output. Manufacturers are now trying to standardise the design and production of PV modules with an output of 700 W+. The proposed module dimensions are 2384 mm × 1303 mm.

### *3.8. PV Module Components*

PV cells are usually not used separately, as they have low power and voltage. In order to produce higher voltage and power, it is necessary to connect several cells in series (and in parallel) to form a PV module. It is very important that the PV module has high efficiency.

Enhancing the efficiency of Si-based PV modules requires not only enhancing solar cell layout and manufacturing technology but also improving the other materials needed to assembly PV modules (Figure 6). PV cells have just as important a role in PV modules as the PV cells.

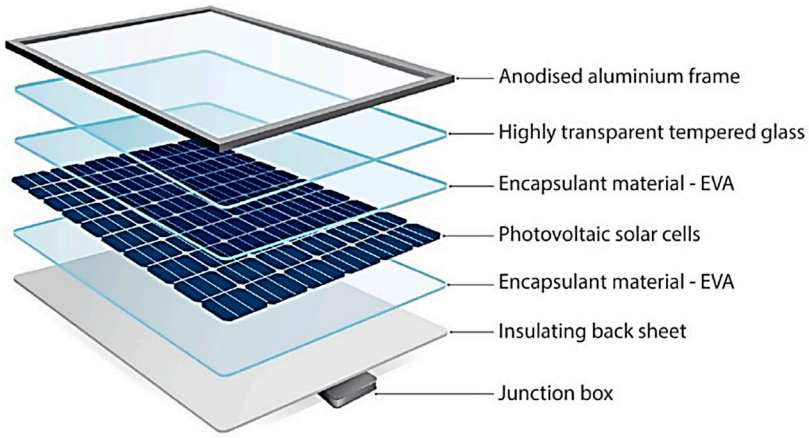


**Figure 6.** PV module components (with the permission of GSES).

#### 3.8.1. The Backsheet

The backsheet is applied to the back of the solar module in the form of a protective film or coating. The materials of which the backsheet is made must protect the PV module from the penetration of UV radiation, water moisture and air pollutants [109,110]. A large part

of the surface of the cells is covered with metal, and all the connecting elements are made of metal, which corrodes when exposed to moisture. To ensure the continuous performance of the module, adequate electrical insulation is required, as several cells are connected in series, resulting in high operating voltages [111].

Polyester (PET) is often used as a backsheet material because it is inexpensive. However, PET is hydrolysed due to the hydrolysable ester bonds in the backbone. Unfortunately, the hydrolysis of PET leads to polymer degradation, which deteriorates mechanical properties, increases embrittlement and reduces UV resistance. Anti-hydrolysis additives, such as phosphoric acid esters or chemicals based on carbodiimide, are occasionally added to PET to prevent hydrolysis. Unfortunately, this process for carbodiimide is complicated, and production costs are high [112]. PET is frequently placed in between two UV-resistant layers during the lamination process to solve this issue. The most common type of backsheet is an opaque multilayer polymer film on the back of a module. The multilayer structure consists of a weatherproof layer facing the air, a core layer for electrical insulation and a layer facing the cells to ensure adhesion to the cells. However, the UV stability of PET is quite poor, so it is not suitable as a self-sufficient substrate material.

Due to their multi-layer structure, backsheets offer enormous potential for technical and economic optimisation. Innovations in the field of backsheets are basically nothing more than a combination of different chemical compositions of polymers. This has always been the case in the development of backsheets throughout history. Polyvinylidene fluoride (PVDF), often known by its trade name Kynar or polyvinyl fluoride (PVF), was considered necessary as an outer protective layer for the reliability of the module and remained the leading backsheet structure for ten years.

However, due to the high demand from the battery segment, PVDF has experienced a huge price increase since 2022, which has been the main reason for many technical–commercial developments in the backsheet area. As a result, the market is replacing the films with coatings (such backsheets are commonly abbreviated as CPC, where "C" stands for coatings of both types, and "P" stands for PET core) and partially moving to non-fluoropolymers [113], as shown in Figure 7. Due to the increasing application of bifacial technology in community solar, a segment that primarily favours the glass-to-glass structure, black backsheets are becoming increasingly popular.

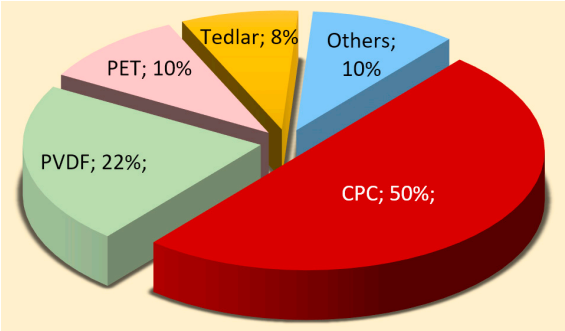


**Figure 7.** Technology share of backsheet structures in 2022 (based on data from [113]).

Sustainability, low carbon footprint and recyclability are factors that have also become attractive to Chinese backsheet manufacturers.

From a technological point of view, the most important trend is the development of transparent backsheets. Glass is becoming a strong competitor for conventional backsheet materials, as it is transparent, offers an extended warranty on module performance and is competitively priced.

Clear backsheets with black mesh that mimic the look of an all-black module are becoming increasingly popular in the growing US residential market. Manufacturers claim that the latest generation of transparent backsheets have the same protective properties as

glass but offer a better energy return due to better heat dissipation and self-cleaning, as well as being lighter [114].

PVDF and CPC have swapped their market positions in the last two years. PVDF's share has fallen from around 55% to 22%, while CPC has increased its share from 13% to 50% [113] (Figure 7).

Co-extruded backsheets based on polypropylene (PP) have recently been developed and successfully launched on the market. Co-extrusion as a new technology challenges the traditional approach to backsheet production by innovating in two areas—production and material. Firstly, it removes the lamination process and the use of adhesives and enables the production of multilayers directly from resins. Theoretically, the technology enables the production of a multilayer structure from different polymers. However, in the current context, a co-extruded backsheet usually uses a single polymer base (PP) but still consists of three layers. Similar to the different layers of a backboard, each of these layers is intended for a different purpose, but the process is glue-free. An important factor is the cost savings resulting from the superior performance of PP and the co-extrusion process itself. Another important factor is sustainability. PP is largely and highly recyclable. The higher reflectivity of the PP backsheet compared to a PET-based reference laminate resulted in a performance increase of 1.5 to 2.5%. The PP backsheet has so far proven to be extremely stable and shows no serious material changes and cracks even after prolonged exposure to temperature, moisture and radiation [109]. In addition, co-extruded PP backsheets are less rigid and more flexible than laminated backsheets [115].

The PV industry is commercialising advanced cell architectures such as TOPCon, HJTs and IBCs. Some of these technologies are more sensitive to moisture ingress compared to standard PERCs. Backsheet manufacturers are now introducing products with water vapour transmission technology (WVTR). These laminates are specifically designed for HJT cells and floating systems with all types of cells. An important feature of the product is that the backsheet structure does not use an aluminium sheet to achieve low WVTR values [113].

Interestingly, some backsheet manufacturers are working on polymer-based front sheets to replace glass. DuPont, for example, has launched a Tedlar-based front sheet, while other manufacturers offer such front sheets for flexible modules. These front films have high transparency and good UV resistance. Flexible modules with polymer front films weigh less than 5 $kg/m^2$ compared to modules for the BIPV market and for special roof projects that require low weight [113].

#### 3.8.2. Encapsulation

Encapsulation is an essential tool to ensure the stability of the operation of photovoltaic cells, to prevent degradation due to weathering (moisture, UV light, oxygen and temperature) and to strengthen mechanical resistance to external agents. To date, various types of polymers have been developed and are commonly used as encapsulation materials, e.g., EVA, PVB, silicone, thermoplastic olefin (TPO) and polyolefin elastomer (POE), with ethylene vinyl acetate (EVA) dominating in the last 30 years. The following qualities of the encapsulating material are necessary for the PV module to have good properties: good physical strength (to shield the cells from outside effects), good adherence to the top and bottom layers, low light absorption, high thermal conductivity, good stability at high temperatures, good stability under UV radiation, optical clarity and low heat resistance [111].

Polyolefin (POE) is increasingly becoming an alternative, especially with the growing popularity of bifacial technology and advanced cell architectures beyond PERCs. Therefore, we divide the encapsulation materials into two categories—EVA and non-EVA. While in the past, encapsulant materials were limited to a single-layer structure, recent developments in polyolefins have led to multilayer encapsulant materials for which there is significant market interest. The typical composition of such a structure is a POE film sandwiched between

two EVA films (EPE), but the reverse structure is also possible. The main motivation is to reduce costs, as POE resin is quite expensive.

The most important trend in the encapsulation segment is compatibility with the rapidly developing cell and module technologies. Encapsulation solutions for solar modules are becoming more and more specific to the cell and module technology and then to the module side. This means that the type of polymer used depends primarily on the cell technology—PERCs, TOPCon, HJTs; the module technology—monofacial or bifacial; and the side of the module—front or back. Sometimes the choice of encapsulation material is also influenced by the type of backsheet [113].

For PERC modules, EVA remains the first choice for the front side. As for the rear side, white EVA is mainly used for monofacial modules with an opaque rear side. For double-layer glass–glass modules, an EPE structure is generally used on the back of the module.

With TOPCon, the passivation and metallisation schemes are the reverse of those of PERCs, i.e., passivation with aluminium oxide takes place on the front side. The front side therefore requires the highest degree of PID protection. The metallisation paste used on the emitter side of the cells is doped with aluminium, so it is more susceptible to corrosion and requires a high barrier against moisture ingress. This also applies to the backside of the TOPCon structure, as it contains a complex passive layer of amorphous silicon and tunnel oxide, which are also sensitive to moisture. With TOPCon, the encapsulant material is usually a pure POE film on the front side and an EPE structure on the back side.

In HJTs, given the hydrophobic nature of the deposited amorphous silicon layers, the encapsulation material should be carefully selected to ensure a high water vapour barrier. The optimisation of the encapsulation material in terms of TCO compatibility is equally important. Encapsulation solutions that support busless interconnection with integrated film are also in demand. The choice could be between POE and EPE on the front and rear side.

One of the most interesting innovations in the field of encapsulation is related to HJTs and their low UV absorption. A wavelength transmission technology has been developed that converts UV light into blue or red light to improve the output power of HJT modules. The film increases the output of the M6 HJT solar module with 60 cells by more than 5 W and can be up to 7 W for larger modules. The power increase is about 1.5% [113]. Global market shares of encapsulations materials in 2022 are shown in Figure 8.

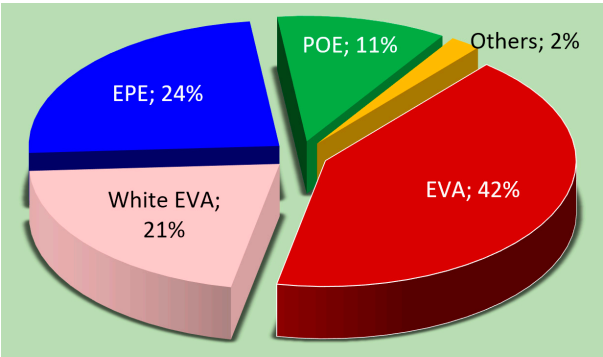


**Figure 8.** Market shares of encapsulation materials in 2022 (based on data from [113]).

## 4. Conclusions

This study provides an overview of the development of Si-based PV cell technology, the latest market trends, research directions and investment decisions and helps stakeholders to make investment decisions and young researchers to identify their research areas.

The production of MG-Si from quartz raw material in large industrial furnaces requires significant electricity consumption, in the range of 10–13 MWh per tonne. Optimisation strategies include using different carbonaceous materials, optimising the proportion of raw materials and improving the efficiency of the furnace design by utilising the thermal

exergy of the waste gases. Recycling PV modules can also reduce energy consumption and $CO_2$ emissions.

High-purity SG-Si is mainly produced using the Siemens process. The author believes that a further reduction in the cost of SG-Si is possible by reducing energy consumption, making better use of waste heat, reducing input costs for MG-Si and other materials, recycling $H_2$, HCl, chlorosilane, etc. and further automating the process to reduce labour. While the Siemens process is still the leader in poly-Si production, the alternative FBR method offers some opportunities to increase efficiency and profitability.

The CZ method is a process for obtaining single crystals from Si. It requires long downtimes and strict control of the process parameters. The alternative FZ method has a lower content of impurities in Si crystals. FZ wafers have a more uniform dopant distribution, which ensures consistent electrical properties and minimises crystal defects. However, the FZ process is associated with high production costs and lower throughput, making it less suitable for mass production. Researchers are investigating hybrid approaches that combine the advantages of the FZ and CZ processes.

Wafers are produced using two common processes: DWS and DWA. DWA reduces scratches and dents on the surface of the wafer. The predominant process is DWS, although costs can be reduced by replacing PEG with water-based liquids. Panel qualities such as thickness variation, roughness, saw damage and fracture resistance need to be improved. Higher diamond wire speeds, thinner wafers, lower cutting losses, higher recycling rates and lower costs for consumables will lead to savings.

Solar cell manufacturing has evolved significantly since the 1950s, with various technologies aimed at increasing efficiency and reducing costs. Understanding the losses that affect cell efficiency is critical.

Optical losses in PV cells reduce the short-circuit current and the light that does not generate electron–hole pairs. To reduce losses, textured or roughened front surfaces, increased effective path length, the minimisation of top contact coverage and anti-reflective coatings are recommended. Ohmic losses in semiconductor materials cause voltage drops, lower efficiency and a lower fill factor in photovoltaic cells. Strategies to reduce these losses include increased busbar thickness, materials with lower contact resistance and advanced cell designs. Recombination occurs at the cell surface, in the bulk and near the p–n junction, and minimising these losses is critical for optimal PV cell performance.

PERC technology improves efficiency and light absorption in solar cells through the use of passivation and reflection layers but is sensitive to shadows.

TOPCon, an advanced N-type Si cell architecture, uses a thin layer of insulating material between the metal contact and the solar cell. This improves electron transport and collection, reduces the recombination rate and ensures a longer lifetime, making it ideal for low-light areas. TOPCon technology improves the surface preparation of PV cells by eliminating damage and reducing reflections. It eliminates etching damage and reduces chemical consumption. TOPCon uses a customised texturing process with a specially developed additive that results in a different pyramid shape and reduces water consumption.

Anti-reflective coatings (ARCs) are critical in solar cells for efficient operation, as they improve light absorption and reduce reflection losses. Current trends include thin-film AR coatings, a gradient refractive index structure (GRIN), a high–low–high–low refractive index structure (HLHL) and the embedding of nanoparticles.

Metal contacts are essential for the production of efficient crystalline Si PV cells. Screen-printed Ag front and Al back metal contacts are widely used. To achieve material sustainability, the PV industry needs to reduce Ag consumption per cell. Alternative solutions include replacing silver with aluminium or copper, using high-temperature copper pastes and enacting laser-assisted burning of the contacts.

IBC solar cells are a sophisticated technology that improves the efficiency of PV modules by rearranging the components. An anti-reflective layer and interdigitated layers enable the separation of electron–hole pairs. IBCs are more complex and expensive to man-

ufacture than conventional Al-BSF cells, but their lower series resistance and decoupling make them valuable for high-efficiency solar applications.

HJTs use a crystalline Si base with ultra-thin amorphous Si layers, which increases efficiency and reduces recombination. They have a low temperature coefficient, ideal for hot climates, and a high bifaciality factor.

Multi-busbars (MBBs) are increasingly being used to improve cell efficiency. They replace traditional strip busbars with thin wire or micro-wire busbars and allow up to 21 busbars to be accommodated in 210 mm cells.

Shingle cells are a new solar module design that uses thin strips of cells that lay horizontally or vertically across the module. This design covers a larger area and reduces power losses. In addition, the cells can be connected in parallel, which reduces shading effects. However, shingle technology has a 2–8% higher silicon consumption rate and additional process steps.

The use of half-size solar cells instead of full-size square cells reduces electrical losses, increases efficiency and reduces hot spots. This design offers 2–4% more power but has a slightly higher price.

Manufacturers are standardising the design and production of PV modules for 700 W+ output by moving from the standard wafer size of 156 mm to larger wafer sizes of 166 mm, 182 mm and 210 mm to increase output.

There have also been some changes to important components for the production of backsheets and encapsulation. The high cost of PVDF has led to a shift in coatings and non-fluoropolymers. Black backsheets are becoming more popular due to bifacial technology in community solar installations. Transparent backsheets offer an extended warranty and competitive pricing. Co-extruded polypropylene backsheets have been developed for cost saving and sustainability reasons.

Common encapsulating polymers include EVA, PVB, silicone, TPO and POE, which is becoming an alternative due to its advanced cellular architecture.

As a final assessment, it can be said that the PV industry has a good development trend in the direction of achieving a "green economy" and the sustainability of the energy production system.

**Funding:** This research received no external funding.

**Institutional Review Board Statement:** Not applicable.

**Informed Consent Statement:** Not applicable.

**Data Availability Statement:** Data are contained within the article.

**Conflicts of Interest:** The author declares no conflicts of interest.

## References

1. Zaidi, B. Introductory Chapter: Introduction to Photovoltaic Effect. In *Solar Panels and Photovoltaic Materials*; Zaidi, B., Ed.; IntechOpen: Rijeka, Yugoslavia, 2018.
2. Hallam, B.; Kim, M.; Underwood, R.; Drury, S.; Wang, L.; Dias, P. A Polysilicon Learning Curve and the Material Requirements for Broad Electrification with Photovoltaics by 2050. *Sol. RRL* **2022**, *6*, 2200458. [CrossRef]
3. Xakalashe, B.S.; Tangstad, M. Silicon Processing: From Quartz to Crystalline Silicon Solar Cells. In Proceedings of the Southern African Pyromethallurgy International Conference, Johannesburg, South Africa, 6–9 March 2011.
4. Takla, M.; Kamfjord, N.E.; Tveit, H.; Kjelstrup, S. Energy and Exergy Analysis of the Silicon Production Process. *Energy* **2013**, *58*, 138–146. [CrossRef]
5. Wen, J.; Zhang, H.; Chen, Z.; Zhang, Z.; Ma, W.; Wu, J. Exergy Analysis of Silicon Metallurgy in 22.5 MVA Submerged Arc Furnaces. *Silicon* **2023**, *15*, 1897–1912. [CrossRef]
6. Chen, Z.; Zhou, S.; Ma, W.; Deng, X.; Li, S.; Ding, W. The Effect of the Carbonaceous Materials Properties on the Energy Consumption of Silicon Production in the Submerged Arc Furnace. *J. Clean. Prod.* **2018**, *191*, 240–247. [CrossRef]
7. Wang, X.; Chen, Z.; Ma, W.; Wen, J. Exergy Efficiency and Energy Analysis of Silicon Production Using Coffee Husks as a Carbon Material. *Silicon* **2023**, *15*, 7965–7978. [CrossRef]
8. Chen, Z.; Ma, W.; Wei, K.; Li, S.; Ding, W. Effect of Raw Materials on the Production Process of the Silicon Furnace. *J. Clean. Prod.* **2017**, *158*, 359–366. [CrossRef]

9. Bošnjaković, M.; Santa, R.; Crnac, Z.; Bošnjaković, T. Environmental Impact of PV Power Systems. *Sustainability* **2023**, *15*, 11888. [CrossRef]
10. Satpathy, R.; Pamuru, V. Chapter 3—Silicon Wafer Manufacturing Process. In *Solar PV Power*; Satpathy, R., Pamuru, V., Eds.; Academic Press: Cambridge, MA, USA, 2021; pp. 53–70, ISBN 978-0-12-817626-9.
11. Zhao, Y.; Wei, K.; Yang, S.; Ma, W.; Xu, C. Study on the Removal Mechanism of Iron Impurities in Raw Coal for Metallurgical-Grade Silicon Smelting. *Silicon* **2023**, *15*, 3931–3943. [CrossRef]
12. Zhang, H.; Chen, Z.; Ma, W.; Cao, S.; Jiang, K.; Zhu, Y. The Effect of Silica and Reducing Agent on the Contents of Impurities in Silicon Produced. *Silicon* **2022**, *14*, 2779–2792. [CrossRef]
13. Chen, Y.; Liu, Y.; Wang, X.; Li, K.; Chen, P. Preparation of High Purity Crystalline Silicon by Electro-Catalytic Reduction of Sodium Hexafluorosilicate with Sodium below 180 °C. *PLoS ONE* **2014**, *9*, e105537. [CrossRef]
14. Zhou, Q.; Wu, J.; Ma, W.; Chen, Z.; Lei, Y.; Wei, K. Boron Removal from Industrial Silicon by Combined Slagging and Acid Leaching Treatment Technology. *JOM* **2020**, *72*, 2670–2675. [CrossRef]
15. Lei, Y.; Ma, W.; Wu, J.; Wei, K.; Li, S.; Morita, K. Impurity Phases and Their Removal in Si Purification with Al–Si Alloy Using Transition Metals as Additives. *J. Alloys Compd.* **2018**, *734*, 250–257. [CrossRef]
16. Han, S.; Tan, N.; Wei, K.; Ma, W. Electromagnetic Separation of Silicon from Metallurgical-Grade Silicon Refined Slag during the Remelting Process. *Sep. Purif. Technol.* **2022**, *280*, 119815. [CrossRef]
17. Kong, J.; Gao, S.; Liu, Y.; Jin, X.; Wei, D.; Jiang, S.; Ye, K.; Wang, J.; Xing, P.; Luo, X. Recycling of Carbonized Rice Husk for Producing High Purity Silicon by the Combination of Electric Arc Smelting and Slag Refining. *J. Hazard. Mater.* **2019**, *380*, 120827. [CrossRef] [PubMed]
18. Philipson, H.; Blandhol, K.; Engvoll, K.; Djupvik, V.; Wallin, M.; Tranell, G.; Haarberg, T. Preliminary Techno-Economic Considerations of the Sisal Process—Closing Materials Loops through Industrial Symbiosis. In *Proceedings of the Silicon for the Chemical & Solar Industry XVI, Online, 14–16 June 2022*; Norwegian University of Science and Technology (NTNU): Trondheim, Norway, 2022; ISBN 978-82-692919-0-2. [CrossRef]
19. Philipson, H.; Solbakk, G.L.; Wallin, M.; Einarsrud, K.E.; Tranell, G. Innovative Utilization of Aluminum-Based Secondary Materials for Production of Metallurgical Silicon and Alumina-Rich Slag. In Proceedings of the Light Metals 2022; Eskin, D., Ed.; Springer International Publishing: Cham, Switzerland, 2022; pp. 1038–1045.
20. Woodhouse, M.; Smith, B.; Ramdas, A.; Margolis, R. *Crystalline Silicon Photovoltaic Module Manufacturing Costs and Sustainable Pricing: 1H 2018 Benchmark and Cost Reduction Roadmap*; National Renewable Energy Laboratory: Golden, CO, USA, 2019; pp. 1–46.
21. Ramírez-Márquez, C.; Martín, M. Chapter 10—Photovoltaic Solar Energy. In *Sustainable Design for Renewable Processes*; Martín, M., Ed.; Elsevier: Amsterdam, The Netherlands, 2022; pp. 397–439, ISBN 978-0-12-824324-4.
22. Alcántara-Maciel, F.D.; Casillas-Céspedes, V.E.; López-García, J.A.; Cabrera-Ruiz, J.; Marquez, C.R.; Alcántara-Ávila, J.R. Economic Optimization of a Reactive Distillation Column with Multiple Reactive Sections for Silane Production. In Proceedings of the 32nd European Symposium on Computer Aided Process Engineering, Toulouse, France, 12–15 June 2022; Montastruc, L., Negny, S., Eds.; Computer Aided Chemical Engineering. Elsevier: Amsterdam, The Netherlands, 2022; Volume 51, pp. 475–480.
23. Ramos, A.; Filtvedt, W.O.; Lindholm, D.; Ramachandran, P.A.; Rodríguez, A.; del Cañizo, C. Deposition Reactors for Solar Grade Silicon: A Comparative Thermal Analysis of a Siemens Reactor and a Fluidized Bed Reactor. *J. Cryst. Growth* **2015**, *431*, 1–9. [CrossRef]
24. Yadav, S.; Chattopadhyay, K.; Singh, C.V. Solar Grade Silicon Production: A Review of Kinetic, Thermodynamic and Fluid Dynamics Based Continuum Scale Modeling. *Renew. Sustain. Energy Rev.* **2017**, *78*, 1288–1314. [CrossRef]
25. Yang, D. *Handbook of Photovoltaic Silicon*; Springer: Berlin/Heidelberg, Germany, 2019; ISBN 9783662564721.
26. Bernreuter, J. Production Processes: Siemens Process, Fluidized Bed Reactor, Upgraded Silicon Metal. Available online: https://www.bernreuter.com/polysilicon/production-processes/ (accessed on 10 April 2024).
27. Möller, H.J. Wafer Processing. In *Handbook of Photovoltaic Silicon*; Yang, D., Ed.; Springer: Berlin/Heidelberg, Germany, 2019; pp. 269–309, ISBN 978-3-662-56472-1.
28. Masson, G.; de I'Epine, M.; Kaizuka, I. *Trends in Photovoltaic Applications, Task 1 Strategic PV Analysis and Outreach, Report Iea Pvps T1-43: 2022*; IEA PVPS: Rheine, Germany, 2023.
29. He, Y.; Ma, W.; Xing, A.; Xu, P.; Yang, X. A High-Efficiency and Energy-Saving Method for Purifying Industrial Silicon for Silicone Use. *Silicon* **2023**, *15*, 2597–2612. [CrossRef]
30. Jiang, L.; Fieselmann, B.F.; Chen, L.; Mixon, D. Fluidized Bed Process with Silane. In *Handbook of Photovoltaic Silicon*; Yang, D., Ed.; Springer: Berlin/Heidelberg, Germany, 2017; pp. 1–40, ISBN 978-3-662-52735-1.
31. Fischer, M.; Michael Woodhouse, P.B.; Trube, J. *International Technology Roadmap for Photovoltaic (ITRPV) 2022 Results*; ETIP PV Publications: Frankfurt am Main, Germany, 2022.
32. Prakash, V.; Agarwal, A.; Mussada, E.K. Processing Methods of Silicon to Its Ingot: A Review. *Silicon* **2019**, *11*, 1617–1634. [CrossRef]
33. Yu, X.; Yang, D. Growth of Crystalline Silicon for Solar Cells: Czochralski Si. In *Handbook of Photovoltaic Silicon*; Yang, D., Ed.; Springer: Berlin/Heidelberg, Germany, 2017; pp. 1–45, ISBN 978-3-662-52735-1.
34. Jeon, H.J.; Park, H.; Koyyada, G.; Alhammadi, S.; Jung, J.H. Optimal Cooling System Design for Increasing the Crystal Growth Rate of Single-Crystal Silicon Ingots in the Czochralski Process Using the Crystal Growth Simulation. *Processes* **2020**, *8*, 1077. [CrossRef]

35. Dezfoli, A.R.A. Czochralski (CZ) Process Modification with Cooling Tube in the Response to Market Global Silicon Shortage. *J. Cryst. Growth* **2023**, *610*, 127170. [CrossRef]
36. Sekar, S.; Thamotharan, K.; Manickam, S.; Murugesan, B.; Kakimoto, K.; Perumalsamy, R. A Critical Review of The Process and Challenges of Silicon Crystal Growth for Photovoltaic Applications. *Cryst. Res. Technol.* **2024**, *59*, 2300131. [CrossRef]
37. Riepe, S.; Nold, S.; Brailovsky, P.; Krenckel, P.; Friedrich, L.; Janz, S.; Preu, R. Presented at the 37th European PV Solar Energy Conference and Exhibition. In Proceedings of the 37th European PV Solar Energy Conference and Exhibition, Online, 7–11 September 2020; Fraunhofer Institute for Solar Energy Systems ISE: Lisbon, Portugal, 2020.
38. ITRPV. *International Technology Roadmap for Photovoltaic (ITRPV)—Results 2018*; VDMA: Frankfurt am Main, Germany, 2019.
39. Liu, W.; Chen, S.; Liu, Y.; Wen, Z.; Jiang, F.; Xue, Z.; Wei, X.; Yu, Y. Three-Dimensional Modelling of 300 Mm Czochralski Silicon Crystal Growth with a Transverse Magnetic Field. *CrystEngComm* **2023**, *25*, 3493–3500. [CrossRef]
40. Sturm, F.; Trempa, M.; Schuster, G.; Götz, P.; Wagner, R.; Barroso, G.; Meisner, P.; Reimann, C.; Friedrich, J. Material Evaluation for Engineering a Novel Crucible Setup for the Growth of Oxygen Free Czochralski Silicon Crystals. *J. Cryst. Growth* **2022**, *584*, 126582. [CrossRef]
41. Riemann, H.; Luedge, A. Floating Zone Crystal Growth. In *Crystal Growth of Si for Solar Cells*; Nakajima, K., Usami, N., Eds.; Springer: Berlin/Heidelberg, Germany, 2009; pp. 41–53, ISBN 978-3-642-02044-5.
42. Chen, T.; Tosello, G.; Calaon, M. Multi-Label Oxide Classification in Float-Zone Silicon Crystal Growth Using Transfer Learning and Asymmetric Loss. *J. Intell. Manuf.* **2024**. [CrossRef]
43. Yang, D.; Liang, X.; Yu, X. Silicon Wafer Processing. In *Handbook of Integrated Circuit Industry*; Wang, Y., Chi, M.-H., Lou, J.J.-C., Chen, C.-Z., Eds.; Springer: Singapore, 2024; pp. 1665–1676, ISBN 978-981-99-2836-1.
44. Li, A.; Hu, S.; Zhou, Y.; Wang, H.; Zhang, Z.; Ming, W. Recent Advances in Precision Diamond Wire Sawing Monocrystalline Silicon. *Micromachines* **2023**, *14*, 1512. [CrossRef]
45. Kumar, A.; Melkote, S.N. Diamond Wire Sawing of Solar Silicon Wafers: A Sustainable Manufacturing Alternative to Loose Abrasive Slurry Sawing. *Procedia Manuf.* **2018**, *21*, 549–566. [CrossRef]
46. Sefene, E.M.; Chen, C.-C.A. Multi-Objective Optimization of Energy Consumption, Surface Roughness, and Material Removal Rate in Diamond Wire Sawing for Monocrystalline Silicon Wafer. *Int. J. Adv. Manuf. Technol.* **2023**, *129*, 2563–2576. [CrossRef]
47. Wei, D.; Zhang, Z.; Zhao, Q.; Kong, J.; Zhuang, Y.; Xing, P. Preparation of High-Quality Silicon with Silicon Cutting Waste by a Carbothermal Reduction Method. *Silicon* **2023**, *15*, 6323–6328. [CrossRef]
48. Wei, D.; Zhou, S.; Kong, J.; Zhuang, Y.; Xing, P. Efficient Recycling of Silicon Cutting Waste for Producing High-Quality Si-Fe Alloys. *Environ. Sci. Pollut. Res.* **2023**, *30*, 62355–62366. [CrossRef]
49. Cheng, D.; Gao, Y. Fracture Probability of PV Mono-Si Wafers in Diamond Wire Slicing Due to Coupling of Capillary Adhesion Bending Stress and Sawing Stress. *Mater. Sci. Semicond. Process.* **2024**, *169*, 107880. [CrossRef]
50. Yin, Y.; Gao, Y.; Wang, L.; Zhang, L.; Pu, T. Analysis of Crack-Free Surface Generation of Photovoltaic Polysilicon Wafer Cut by Diamond Wire Saw. *Sol. Energy* **2021**, *216*, 245–258. [CrossRef]
51. Oni, A.M.; Mohsin, A.S.M.; Rahman, M.M.; Hossain Bhuian, M.B. A Comprehensive Evaluation of Solar Cell Technologies, Associated Loss Mechanisms, and Efficiency Enhancement Strategies for Photovoltaic Cells. *Energy Rep.* **2024**, *11*, 3345–3366. [CrossRef]
52. McIntosh, K.R.; Kho, T.C.; Fong, K.C.; Baker-Finch, S.C.; Wan, Y.; Zin, N.; Franklin, E.T.; Wang, D.; Abbott, M.D.; Grant, N.E.; et al. Quantifying the Optical Losses in Back-Contact Solar Cells. In Proceedings of the 2014 IEEE 40th Photovoltaic Specialist Conference (PVSC), Denver, CO, USA, 8–13 June 2014; pp. 115–123.
53. Saive, R. Light Trapping in Thin Silicon Solar Cells: A Review on Fundamentals and Technologies. *Progress. Photovolt. Res. Appl.* **2021**, *29*, 1125–1137. [CrossRef]
54. Shaker, L.M.; Al-Amiery, A.A.; Hanoon, M.M.; Al-Azzawi, W.K.; Kadhum, A.A.H. Examining the Influence of Thermal Effects on Solar Cells: A Comprehensive Review. *Sustain. Energy Res.* **2024**, *11*, 6. [CrossRef]
55. Sun, C.; Zou, Y.; Qin, C.; Zhang, B.; Wu, X. Temperature Effect of Photovoltaic Cells: A Review. *Adv. Compos. Hybrid Mater.* **2022**, *5*, 2675–2699. [CrossRef]
56. Riverola, A.; Mellor, A.; Alonso Alvarez, D.; Ferre Llin, L.; Guarracino, I.; Markides, C.N.; Paul, D.J.; Chemisana, D.; Ekins-Daukes, N. Mid-Infrared Emissivity of Crystalline Silicon Solar Cells. *Sol. Energy Mater. Sol. Cells* **2018**, *174*, 607–615. [CrossRef]
57. Zhu, L.; Raman, A.; Wang, K.X.; Anoma, M.A.; Fan, S. Radiative Cooling of Solar Cells. *Optica* **2014**, *1*, 32–38. [CrossRef]
58. Alves dos Santos, S.A.; Torres, J.P.N.; Fernandes, C.A.F.; Marques Lameirinhas, R.A. The Impact of Aging of Solar Cells on the Performance of Photovoltaic Panels. *Energy Convers. Manag. X* **2021**, *10*, 100082. [CrossRef]
59. Wang, Q.; Wu, W.; Chen, D.; Yuan, L.; Yang, S.; Sun, Y.; Yang, S.; Zhang, Q.; Cao, Y.; Qu, H.; et al. Study on the Cleaning Process of N+-Poly-Si Wraparound Removal of TOPCon Solar Cells. *Sol. Energy* **2020**, *211*, 324–335. [CrossRef]
60. Shravan, K.; Chunduri, M.S. *Market Survey: Solar Cell Production Equipment 2023*; TaiyangNews UG: Duesseldorf, Germany, 2023; ISBN 9783949046186.
61. Fischer, A.; Moldovan, A.; Temmler, J.; Zimmer, M.; Rentsch, J. Development of an Ozone-Based Inline Cleaning and Conditioning Concept. *AIP Conf. Proc.* **2018**, *1999*, 50001. [CrossRef]
62. McIntosh, K.R.; Baker-Finch, S.C. A Parameterization of Light Trapping in Wafer-Based Solar Cells. *IEEE J. Photovolt.* **2015**, *5*, 1563–1570. [CrossRef]

63. McIntosh, K.R.; Allen, T.G.; Baker-Finch, S.C.; Abbott, M.D. Light Trapping in Isotextured Silicon Wafers. *IEEE J. Photovolt.* **2017**, *7*, 110–117. [CrossRef]
64. Huo, C.; Fu, H.; Peng, K.Q. Inverted Pyramid Structures Fabricated on Monocrystalline Silicon Surface with a NaOH Solution. *Heliyon* **2024**, *10*, e23871. [CrossRef] [PubMed]
65. McIntosh, K.R.; Zin, N.; Nguyen, H.T.; Stocks, M.; Franklin, E.; Fong, K.C.; Kho, T.C.; Chong, T.K.; Wang, E.-C.; Ratcliff, T.; et al. Optical Evaluation of Silicon Wafers With Rounded Rear Pyramids. *IEEE J. Photovolt.* **2017**, *7*, 1596–1602. [CrossRef]
66. Liu, H.; Zhao, L.; Diao, H.; Wang, W. High-Performance Texturization of Multicrystalline Silicon Wafer by HF/$HNO_3$/$H_2O$ System Incorporated with $MnO_2$ Particles. *Mater. Sci. Semicond. Process.* **2019**, *101*, 149–155. [CrossRef]
67. Ok, Y.-W.; Tam, A.M.; Huang, Y.-Y.; Yelundur, V.; Das, A.; Payne, A.M.; Chandrasekaran, V.; Upadhyaya, A.D.; Jain, A.; Rohatgi, A. Screen Printed, Large Area Bifacial N-Type Back Junction Silicon Solar Cells with Selective Phosphorus Front Surface Field and Boron Doped Poly-Si/SiOx Passivated Rear Emitter. *Appl. Phys. Lett.* **2018**, *113*, 263901. [CrossRef]
68. Park, H.; Park, H.; Park, S.J.; Bae, S.; Kim, H.; Yang, J.W.; Hyun, J.Y.; Lee, C.H.; Shin, S.H.; Kang, Y.; et al. Passivation Quality Control in Poly-Si/SiOx/c-Si Passivated Contact Solar Cells with 734 MV Implied Open Circuit Voltage. *Sol. Energy Mater. Sol. Cells* **2019**, *189*, 21–26. [CrossRef]
69. Yoshikawa, K.; Kawasaki, H.; Yoshida, W.; Irie, T.; Konishi, K.; Nakano, K.; Uto, T.; Adachi, D.; Kanematsu, M.; Uzu, H.; et al. Silicon Heterojunction Solar Cell with Interdigitated Back Contacts for a Photoconversion Efficiency over 26%. *Nat. Energy* **2017**, *2*, 17032. [CrossRef]
70. Richter, A.; Benick, J.; Feldmann, F.; Fell, A.; Hermle, M.; Glunz, S.W. N-Type Si Solar Cells with Passivating Electron Contact: Identifying Sources for Efficiency Limitations by Wafer Thickness and Resistivity Variation. *Sol. Energy Mater. Sol. Cells* **2017**, *173*, 96–105. [CrossRef]
71. Ingenito, A.; Nogay, G.; Jeangros, Q.; Rucavado, E.; Allebé, C.; Eswara, S.; Valle, N.; Wirtz, T.; Horzel, J.; Koida, T.; et al. A Passivating Contact for Silicon Solar Cells Formed during a Single Firing Thermal Annealing. *Nat. Energy* **2018**, *3*, 800–808. [CrossRef]
72. Richter, A.; Benick, J.; Müller, R.; Feldmann, F.; Reichel, C.; Hermle, M.; Glunz, S.W. Tunnel Oxide Passivating Electron Contacts as Full-Area Rear Emitter of High-Efficiency p-Type Silicon Solar Cells. *Progress. Photovolt. Res. Appl.* **2018**, *26*, 579–586. [CrossRef]
73. Steinhauser, B.; Polzin, J.-I.; Feldmann, F.; Hermle, M.; Glunz, S.W. Excellent Surface Passivation Quality on Crystalline Silicon Using Industrial-Scale Direct-Plasma TOPCon Deposition Technology. *Sol. RRL* **2018**, *2*, 1800068. [CrossRef]
74. Krieg, K.; Mack, S.; Vollmer, J.; Dannenberg, T.; Brunner, D.; Zimmer, M. Wet Chemical Poly-Si(n) Wrap-around Removal for TOPCon Solar Cells. *EPJ Photovolt.* **2024**, *15*, 9. [CrossRef]
75. Schmidt, J.; Peibst, R.; Brendel, R. Surface Passivation of Crystalline Silicon Solar Cells: Present and Future. *Sol. Energy Mater. Sol. Cells* **2018**, *187*, 39–54. [CrossRef]
76. ur Rehman, A.; Iqbal, M.Z.; Bhopal, M.F.; Khan, M.F.; Hussain, F.; Iqbal, J.; Khan, M.; Lee, S.H. Development and Prospects of Surface Passivation Schemes for High-Efficiency c-Si Solar Cells. *Sol. Energy* **2018**, *166*, 90–97. [CrossRef]
77. Padhamnath, P.; Choi, W.-J.; De Luna, G.; Arcebal, J.D.; Rohatgi, A. Design, Development and Analysis of Large-Area Industrial Silicon Solar Cells Featuring a Full Area Polysilicon Based Passivating Contact on the Rear and Selective Passivating Contacts on the Front. *Sol. Energy Mater. Sol. Cells* **2023**, *256*, 112351. [CrossRef]
78. Ullah, H.; Czapp, S.; Szultka, S.; Tariq, H.; Qasim, U.B.; Imran, H. Crystalline Silicon (c-Si)-Based Tunnel Oxide Passivated Contact (TOPCon) Solar Cells: A Review. *Energies* **2023**, *16*, 715. [CrossRef]
79. Glunz, S.W.; Steinhauser, B.; Polzin, J.-I.; Luderer, C.; Grübel, B.; Niewelt, T.; Okasha, A.M.O.M.; Bories, M.; Nagel, H.; Krieg, K.; et al. Silicon-Based Passivating Contacts: The TOPCon Route. *Progress. Photovolt. Res. Appl.* **2023**, *31*, 341–359. [CrossRef]
80. Mack, S.; Kafle, B.; Tessmann, C.; Krieg, K.; Bashardoust, S.; Lohmüller, E.; Belledin, U.; Saint-cast, P.; Höffler, H.; Ourinson, D.; et al. Status and Perspective of Industrial TOPCon Solar Cell Development at Fraunhofer ISE. In Proceedings of the 8th World Conference on Photovoltaic Energy Conversion (WCPEC), Milano, Italy, 26–30 September 2022; pp. 26–30.
81. Law, A.M.; Jones, L.O.; Walls, J.M. The Performance and Durability of Anti-Reflection Coatings for Solar Module Cover Glass—Review. *Sol. Energy* **2023**, *261*, 85–95. [CrossRef]
82. Ji, C.; Liu, W.; Bao, Y.; Chen, X.; Yang, G.; Wei, B.; Yang, F.; Wang, X. Recent Applications of Antireflection Coatings in Solar Cells. *Photonics* **2022**, *9*, 906. [CrossRef]
83. Mercy, P.A.M.; Wilson, K.S.J. Comparative Study of Polarization-Dependent Conversion Efficiency of GaAs and Si Solar Cells at Oblique Incident Angles Using Surface DLAR Coating of $MgF_2$/ZnSe. *Cryst. Res. Technol.* **2024**, *59*, 2300035. [CrossRef]
84. Richards, B.S.; Rowlands, S.F.; Honsberg, C.B.; Cotter, J.E. $TiO_2$ DLAR Coatings for Planar Silicon Solar Cells. *Progress. Photovolt. Res. Appl.* **2003**, *11*, 27–32. [CrossRef]
85. Shanmugam, N.; Pugazhendhi, R.; Madurai Elavarasan, R.; Kasiviswanathan, P.; Das, N. Anti-Reflective Coating Materials: A Holistic Review from PV Perspective. *Energies* **2020**, *13*, 2631. [CrossRef]
86. Mehta, V.; Conkel, C.; Cochran, A.; Ravindra, N.M. Materials for Antireflection Coatings in Photovoltaics—An Overview. In *Proceedings of the TMS 2022 151st Annual Meeting & Exhibition Supplemental Proceedings*; Springer International Publishing: Cham, Switzerland, 2022; pp. 350–365.
87. Phimu, L.K.; Dhar, R.S.; Singh, K.J. Design Optimization of Thickness and Material of Antireflective Layer for Solar Cell Structure. *Silicon* **2022**, *14*, 8119–8128. [CrossRef]

88. Ramos-Carrazco, A.; Berman-Mendoza, D.; Ramirez-Espinoza, R.; Gutierrez, R.G.; Vazquez-Arce, J.L.; Rangel, R.; Melendrez-Amavizca, R.; Bartolo-Pérez, P. $Al_2O_3$/Si NPs Multilayered Antireflective Coating to Enhance the Photovoltaic Performance of Solar Cells. *J. Mater. Sci. Mater. Electron.* **2023**, *34*, 2328. [CrossRef]
89. Balaji, N.; Raval, M.C.; Saravanan, S. Review on Metallization in Crystalline Silicon Solar Cells. In *Solar Cells*; Nayeripour, M., Mansouri, M., Waffenschmidt, E., Eds.; IntechOpen: Rijeka, Yugoslavia, 2019.
90. Voroshazi, E.; Beaucarne, G.; Lossen, J.; Faes, A. Summary of the 11th Workshop on Metallization and Interconnection for Crystalline Silicon Solar Cells. *Sol. Energy Mater. Sol. Cells* **2024**, *269*, 112772. [CrossRef]
91. Dullweber, T.; Tous, L. *Silicon Solar Cell Metallization and Module Technology*, 2022nd ed.; Dullweber, T., Tous, L., Eds.; The Institution of Engineering and Technology: London, UK, 2021; ISBN 9781839531552.
92. Zhang, Y.; Kim, M.; Wang, L.; Verlinden, P.; Hallam, B. Design Considerations for Multi-Terawatt Scale Manufacturing of Existing and Future Photovoltaic Technologies: Challenges and Opportunities Related to Silver{,} Indium and Bismuth Consumption. *Energy Environ. Sci.* **2021**, *14*, 5587–5610. [CrossRef]
93. Ebong, A.; Intal, D.; Huneycutt, S.; Druffel, T.; Dharmadasa, R.; Elmer, K.; Nambo, A. Screen Printable Copper Pastes for Silicon Solar Cells. *Sol. Energy Mater. Sol. Cells* **2024**, *265*, 112633. [CrossRef]
94. Ourinson, D.; Brand, A.; Lorenz, A.; Dhamrin, M.; Tepner, S.; Linse, M.; Göttlicher, N.; Haberstroh, R.; Tsuji, K.; Huyeng, J.D.; et al. Paste-Based Silver Reduction for ITOPCon Rear Side Metallization. *Sol. Energy Mater. Sol. Cells* **2024**, *266*, 112646. [CrossRef]
95. Wenzel, T.; Lorenz, A.; Lohmüller, E.; Auerbach, S.; Masuri, K.; Lau, Y.C.; Tepner, S.; Clement, F. Progress with Screen Printed Metallization of Silicon Solar Cells—Towards 20 Mm Line Width and 20 Mg Silver Laydown for PERC Front Side Contacts. *Sol. Energy Mater. Sol. Cells* **2022**, *244*, 111804. [CrossRef]
96. Wu, X.; Wang, X.; Yang, W.; Nie, J.; Yuan, J.; Khan, M.U.; Ciesla, A.; Sen, C.; Qiao, Z.; Hoex, B. Enhancing the Reliability of TOPCon Technology by Laser-Enhanced Contact Firing. *Sol. Energy Mater. Sol. Cells* **2024**, *271*, 112846. [CrossRef]
97. Zeng, Y.; Peng, C.-W.; Hong, W.; Wang, S.; Yu, C.; Zou, S.; Su, X. Review on Metallization Approaches for High-Efficiency Silicon Heterojunction Solar Cells. *Trans. Tianjin Univ.* **2022**, *28*, 358–373. [CrossRef]
98. Lakhe, A.; Upadhye, S.; Goshikwar, Y.; Lakhe, T. Study of Modern Solar Technologies: PERC and HJT. *Int. Res. J. Eng. Technol.* **2022**, *9*, 2035–2043.
99. Kopecek, R.; Buchholz, F.; Mihailetchi, V.D.; Libal, J.; Lossen, J.; Chen, N.; Chu, H.; Peter, C.; Timofte, T.; Halm, A.; et al. Interdigitated Back Contact Technology as Final Evolution for Industrial Crystalline Single-Junction Silicon Solar Cell. *Solar* **2023**, *3*, 1–14. [CrossRef]
100. Wang, P.; Sridharan, R.; Ng, X.R.; Ho, J.W.; Stangl, R. Development of TOPCon Tunnel-IBC Solar Cells with Screen-Printed Fire-through Contacts by Laser Patterning. *Sol. Energy Mater. Sol. Cells* **2021**, *220*, 110834. [CrossRef]
101. Chen, N.; Rudolph, D.; Peter, C.; Zeman, M.; Isabella, O.; Rosen, Y.; Grouchko, M.; Shochet, O.; Mihailetchi, V.D. Thermal Stable High-Efficiency Copper Screen Printed Back Contact Solar Cells. *Sol. RRL* **2023**, *7*, 2200874. [CrossRef]
102. Liu, Y.; Li, Y.; Wu, Y.; Yang, G.; Mazzarella, L.; Procel-Moya, P.; Tamboli, A.C.; Weber, K.; Boccard, M.; Isabella, O.; et al. High-Efficiency Silicon Heterojunction Solar Cells: Materials, Devices and Applications. *Mater. Sci. Eng. R Rep.* **2020**, *142*, 100579. [CrossRef]
103. Bošnjaković, M.; Stojkov, M.; Katinić, M.; Lacković, I. Effects of Extreme Weather Conditions on PV Systems. *Sustainability* **2023**, *15*, 16044. [CrossRef]
104. Joshi, A.; Khan, A.; SP, A. Comparison of Half Cut Solar Cells with Standard Solar Cells. In Proceedings of the 2019 Advances in Science and Engineering Technology International Conferences (ASET), Dubai, United Arab Emirates, 26 March–10 April 2019; pp. 1–3.
105. Von Kutzleben, D.; Rößler, T.; Mittag, M.; Weber, J.; Sigdel, S.; Klasen, N.; Zahn, P.; Kraft, A.; Neuhaus, H. Development of Shingle Matrix Technology for Integrated Pv Applications. In Proceedings of the WCPEC-8, 8th World Conference on Photovoltaic Energy Conversion, Milan, Italy, 26–30 September 2022.
106. Mouhib, E.; Rodrigo, P.M.; Micheli, L.; Fernández, E.F.; Almonacid, F. Quantifying the Rear and Front Long-Term Spectral Impact on Bifacial Photovoltaic Modules. *Sol. Energy* **2022**, *247*, 202–213. [CrossRef]
107. Mouhib, E.; Fernández-Solas, Á.; Pérez-Higueras, P.J.; Fernández-Ocaña, A.M.; Micheli, L.; Almonacid, F.; Fernández, E.F. Enhancing Land Use: Integrating Bifacial PV and Olive Trees in Agrivoltaic Systems. *Appl. Energy* **2024**, *359*, 122660. [CrossRef]
108. Mouhib, E.; Micheli, L.; Almonacid, F.M.; Fernández, E.F. Overview of the Fundamentals and Applications of Bifacial Photovoltaic Technology: Agrivoltaics and Aquavoltaics. *Energies* **2022**, *15*, 8777. [CrossRef]
109. Oreski, G.; Eder, G.C.; Voronko, Y.; Omazic, A.; Neumaier, L.; Mühleisen, W.; Ujvari, G.; Ebner, R.; Edler, M. Performance of PV Modules Using Co-Extruded Backsheets Based on Polypropylene. *Sol. Energy Mater. Sol. Cells* **2021**, *223*, 110976. [CrossRef]
110. Gambogi, W.; Heta, Y.; Hashimoto, K.; Kopchick, J.; Felder, T.; MacMaster, S.; Bradley, A.; Hamzavytehrany, B.; Garreau-Iles, L.; Aoki, T.; et al. A Comparison of Key PV Backsheet and Module Performance from Fielded Module Exposures and Accelerated Tests. *IEEE J. Photovolt.* **2014**, *4*, 935–941. [CrossRef]
111. Kim, D.; Lim, H.; Kim, S.H.; Lee, K.N.; You, J.; Ryu, D.Y.; Kim, J. Recent Developments of Polymer-Based Encapsulants and Backsheets for Stable and High-Performance Silicon Photovoltaic Modules: Materials Nanoarchitectonics and Mechanisms. *J. Mater. Chem. A* **2024**, *12*, 7452–7469. [CrossRef]
112. Ottersböck, B.; Oreski, G.; Pinter, G. Correlation Study of Damp Heat and Pressure Cooker Testing on Backsheets. *J. Appl. Polym. Sci.* **2016**, *133*, 44230. [CrossRef]

113. Schmela, M.; Chunduri, S.K. *Market Survey—Backsheets and Encapsulation 2020*; TaiyangNews UG: Duesseldorf, Germany, 2020; ISBN 9783949046094.
114. Smith, S.; Mitterhofer, S.; Moffitt, S.L.; Jhang, S.-S.; Watson, S.S.; Sung, L.-P.; Gu, X. Long-Term Durability of Transparent Backsheets for Bifacial Photovoltaics: An in-Depth Degradation Analysis. *Sol. Energy Mater. Sol. Cells* **2023**, *256*, 112309. [CrossRef]
115. Oreski, G.; Barretta, C.; Macher, A.; Eder, G.; Neumaier, L.; Feichtner, M.; Aarnio-Winterhof, M. Investigation of the Crack Propensity of Co-Extruded Polypropylene Backsheet Films for Photovoltaic Modules. *Sol. Energy Mater. Sol. Cells* **2023**, *259*, 112438. [CrossRef]